Recent advances in environmental science and engineering applications of cellulose nanocomposites

Asifur Rahman,[a,b] Wei Wang,[a,b] Govindaraj Divyapriya,[a,b] Seju Kang,[a,b] Peter J. Vikesland[a,b*]

[a]Department of Civil and Environmental Engineering, Virginia Tech, Blacksburg, Virginia;

[b]Virginia Tech Institute of Critical Technology and Applied Science (ICTAS) Sustainable Nanotechnology Center (VTSuN), Blacksburg, Virginia;

* *Corresponding author.* Tel.: +1; fax: +; E-mail address: pvikes@vt.edu (P. Vikesland).
Postal address: 415 Durham Hall, Virginia Tech, Blacksburg 24061, VA, USA

Abstract

Cellulose nanomaterials are low cost, biocompatible and readily combined with other materials to produce nanocomposites with a range of applications. Cellulose nanomaterials have many advantageous properties, including high mechanical and thermal stability, high specific surface area, and biodegradability. The highly flexible cellulose structure can be exploited to transform bulk cellulose into isolated nanostructured fibers that retain the original thermal, mechanical, and optical properties of the bulk material. In this review, we highlight recent advances in the environmental application of cellulose nanocomposites. We introduce the different chemical, mechanical, and biological pathways used for preparation of cellulose nanomaterials. Recent rapid technological advancements in the preparation of cellulose nanocomposites by combining metal nanoparticles, organic polymers, and metal-organic frameworks (MOFs) with cellulose are then discussed. Finally, we summarize the latest progress in the application of cellulose nanocomposites in environmental science and engineering and provide a perspective on the future outlook of cellulose nanocomposites.

Keywords Cellulose nanocomposites; Environmental Sensing, Catalysis, Pollutant Removal, Energy Recovery, Sustainability

Graphical abstract

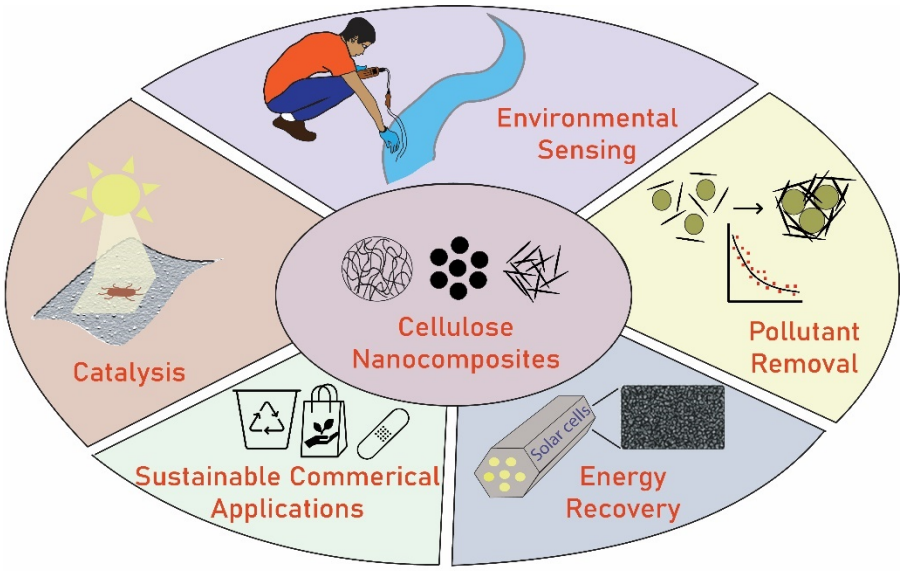

Table of Contents

53 # 1. Introduction

54 The field of nanotechnology is continually evolving and has seen rapid development of a wide
55 range of nanomaterials and nanocomposites with applications in chemistry, chemical and
56 biomedical engineering, physics, materials science, engineering, and beyond (Thomas et al.,
57 2018). Cellulose nanomaterials have attracted interest as biocompatible materials with
58 multifarious applications in science and engineering (Salas et al., 2014; Usov et al., 2015). The
59 presence of highly reactive hydroxyl (-OH) groups on the cellulose surface enables attachment of
60 inorganic metal nanoparticles (NPs; e.g., Au, Ag, Pd, Ni, TiO_2, etc.), organic polymer networks
61 (e.g., alginate, chitosan, β-Cyclodextrin, etc.) and metal organic frameworks (MOFs; e.g.,
62 $Zn_3(BDC)_2$, UiO-66-NH_2, etc.) (Joseph et al., 2020; Kaushik & Moores, 2016; Torres et al., 2019;
63 Yang et al., 2017; Zhang et al., 2018). Because of these advantages, cellulose nanocomposites
64 have been used in a range of applications such as biosensing, drug delivery, catalysis, membrane
65 filtration, and packaging (Carpenter et al., 2015; Jacob et al., 2018; Kaushik & Moores, 2016; Peng
66 et al., 2020; Stark, 2016). Prior reviews have broadly covered the sourcing, synthesis, structural
67 properties, and applications of cellulose nanomaterials (Moon et al., 2011; Thomas et al., 2018;
68 Trache et al., 2017). However, given their facile synthesis and low environmental impact, cellulose
69 nanomaterials have gained special interest in environmental science and engineering (Wei et al.,
70 2014; Li et al., 2021). This review highlights recent advances made in the development of cellulose
71 nanocomposites with a focus on their environmental applications reported in the last 5 to 7 years.
72 The information provided herein is intended to enrich the state of knowledge of environmental
73 science and engineering researchers and engineers and provide an improved understanding of the
74 potential applications of cellulose nanocomposites to address environmental challenges.

Cellulose nanomaterials can exist in different forms depending on the method of preparation. Bulk cellulose is generally used as the parent cellulose material that can be broken into intermediate, smaller cellulose materials by chemical or mechanical processes. Different forms of these products, such as cellulose microfibrils (CMFs), cellulose nanofibrils (CNFs), cellulose microparticles (CMPs), and cellulose microspheres (CMSs) have been described (Figure 1; Dufresne et al., 2000; Fujii et al., 2020; Yu et al., 2021). Cellulose can be further broken up into isolated fibers or crystal structures with varying degrees of crystallinity, these materials are usually referred to as cellulose nanocrystals (CNCs) (Figure 1; Habibi et al., 2010). Bulk cellulose with micro- or nano-fibrillated structure is primarily prepared by mechanical or chemical processing of woody plants, non-agricultural source materials (e.g., rice straw bagasse, cotton stalk fibers, potato peel, etc.), and bacterial laboratory cultures (Adel et al., 2016; Garemark et al., 2020; Li et al., 2017). Previously, bulk cellulose aerogels were produced from native Balsa wood using a top-down synthesis method involving wood cell delignification (Garemark et al., 2020). Among non-agricultural sources, rice straw, bagasse, and cotton stalk biomass have been used to isolate cellulose after chemical delignification (Adel et al., 2016). Bacterial cellulose (BC) is produced by certain species of bacteria (e.g., *Komagataeibacter xylinus*, *Gluconacetobacter xylinus*) in liquid media culture (Li et al., 2017). Due to its facile synthesis and biocompatibility, BC has drawn interest as a viable alternative to plant derived cellulose. Bulk cellulose can be converted to CNCs using different processes or a combination of these processes, as shown in Figure 1. Hydrolysis with inorganic acids (e.g., HCl, H_2SO_4, etc.) is the most widely used method for producing highly crystalline CNCs (Brinkmann et al., 2016). Mechanical treatments, such as electron beam irradiation, followed by high pressure homogenization remain popular methods to produce CNCs despite their high energy requirements. Oxidation and enzyme hydrolysis methods have been

reported as less energy intensive methods that can produce highly crystalline CNCs when followed by post-treatment (e.g., ultrasonication, homogenization, etc.) (Rovera et al., 2018; Zhou et al., 2018). Organic acids and ionic liquids have been promoted as recyclable and mild reaction agents for the 'green' synthesis of CNCs (Fu et al., 2020). Combining multiple processes can sometimes yield CNCs with enhanced reactivity and thermal stability (Pang et al., 2018). Acid hydrolysis and oxidation processes are still most common due to the straightforward synthesis procedures, established protocols and homogenized crystalline products. While other treatment methods (mechanical, enzyme hydrolysis and ionic liquid treatments) offer the use of mild chemicals and low waste generation, research on these methods needs to be further developed for widespread adoption. Furthermore, the selection of a treatment method and the overall performance of the synthesized CNCs is dependent on several factors: cellulose source, the chemicals used for processing, experimental and post-treatment conditions (Moon et al., 2011). Research into the development of novel nanocomposites using CNCs has grown in recent times given their advantageous material properties, such as colloidal and thermal stability, high specific surface area, and homogenous dispersity (Nasseri et al., 2020). Considering the facile synthesis and biodegradability of cellulose nanomaterials, environmental applications of these materials have rapidly increased. The facile tunability of cellulose materials allows for modification into paper-based substrates as templating agents, transparent films, hydrogels, and aerogels.

2. Preparation and properties of cellulose nanocomposites

Cellulose nanomaterials have several characteristics that make them desirable substrates as templating agents for a variety of guest materials. First, the tunable surface of cellulose enables formation of covalent bonds with a range of functional groups (Musino et al., 2021; Stenstad et al., 2008). Secondly, cellulose can be shaped into different types, such as bulk cellulose, CMFs,

121 CNFs, CNCs, etc. by straightforward procedures while retaining similar characteristics, such as
122 high mechanical strength, surface tunability and biocompatibility, irrespective of the cellulose
123 form (Kang et al., 2020; Rusin et al., 2020). The commonly described forms of cellulose found in
124 the literature are CMFs, CNFs and CNCs. Typical properties of these cellulose subunits are
125 summarized in Table 1. Compared to CMFs and CNFs, CNCs are smaller dimension (i.e.,
126 length/width/diameter) isolated structures and hence, possess a greater range of specific surface
127 area for surface modification. Cellulose nanomaterials are commonly surface functionalized with
128 carboxyl (-COOH) groups using TEMPO mediated oxidation, or sulfate half-ester (-O-SO_3H)
129 groups using sulfuric acid hydrolysis. The surface density of these functional groups on cellulose
130 surface is an important measure of the number of surface sites available for guest material binding
131 (Camargos et al., 2021; Johnston et al., 2018; Beck et al., 2015). Cellulose materials possess a high
132 tensile strength that is comparable to other carbon-based materials, such as carbon fiber and carbon
133 nanotubes (Moon et al., 2011). Depending on the surface treatment of the cellulose subunits
134 (CMFs/CNFs/CNCs), widely varying tensile strengths have been reported (Table 1). Lastly,
135 cellulose is considered a cost-effective and environment friendly material due it's nontoxic nature
136 and biodegradability. Commonly produced types of cellulose nanocomposites are discussed in the
137 following sections.

138 *2.1. Cellulose-metal nanoparticle nanocomposites*

139 Metal and metal oxide NPs (e.g., Au, Ag, CuO, Fe, TiO_2) can be combined with cellulose
140 nanomaterials to develop nanocomposites that take advantage of the unique properties of both the
141 guest particles and cellulose. Commonly used techniques of functionalization using metal and
142 metal oxide NPs are: 1) Addition of metal or metal oxide NPs onto the cellulose fibers via
143 reduction of solution-phase metal precursors; 2) direct addition of metal or metal oxide NPs via

144 physical or chemical routes onto the surface or inside the porous cellulose structure; and 3) use of
145 a separate nano-sized coating of metal over the cellulose surface. For example, gold NPs (AuNPs)
146 were deposited on bulk cellulose by reduction of Au^{3+} ions in solution for production of a
147 nanocomposite surface enhanced Raman scattering (SERS) substrate for environmental sensing
148 (Figure 2A; Wei et al., 2015). A mild reducing agent, sodium citrate (Na_3Cit), was used to provide
149 faster reduction of Au^{3+} ions relative to reduction by the surface -OH groups of nanocellulose.
150 Although metal NPs can also be immobilized on the cellulose surfaces by the reducing action of
151 the -OH groups, the use of a reducing agent can perform dual roles of both a reducing agent and a
152 stabilizer for the NPs in solution (Dong et al. 2009, Wei et al., 2015). The highly efficient catalytic
153 properties of Ag, TiO_2, and Pd have been used to incorporate these nanomaterials onto cellulose
154 structures. Recently, porous micro-crystalline cellulose particles were functionalized using
155 carboxylate groups and used as scaffolds for AgNP synthesis by *in situ* reduction of Ag^+ ions
156 (Figure 2B; Fujii et al., 2020). Here, a strong reducing agent, sodium borohydride ($NaBH_4$) was
157 used for fast room temperature reduction, which resulted in formation of AgNPs with diameter
158 <10 nm (Fujii et al., 2020). The resulting spherical cellulose/Ag microparticles are easily dispersed
159 in aqueous suspension as catalytic agents. In another study, BC was used as a substrate for the
160 incorporation of cellulose nanofibril-derived carbon (CDC) and TiO_2 NPs (Li et al., 2020). Here,
161 a BC suspension was used to make a mold that was dried at 40 $^{\circ}$C for 24 hrs to make BC films and
162 then freeze dried for 24 hrs to make BC aerogels. Impressively, the resulting films or aerogels
163 functionalized with CDC/TiO_2 can be washed using sulfuric acid or ethanol for repeated use. Rapid
164 reduction using $NaBH_4$ was also used to incorporate magnetic nano zero-valent iron (nano-ZVIs)
165 particles onto carboxylated CNCs (Bossa et al., 2017). The resulting nanocomposites can be
166 separated from suspension using a magnetic field instead of centrifugation which allows for energy

167 efficiency. Controlling the aggregation and maintaining the homogenous distribution of metal NPs
168 on cellulose surfaces remain major challenges which need optimization of metal concentration
169 (Wei et al., 2015; Fujii et al., 2020; Bossa et al., 2017). Recently, green synthesis approaches that
170 involve one-step fabrication of cellulose nanocomposites were explored. The method involves the
171 use of room temperature ionic liquids for cellulose processing and the simultaneous integration of
172 functionalized NPs (i.e., TiO_2, Fe_3O_4) (Wittmar et al., 2017).

173 ### *2.2. Cellulose-organic polymer nanocomposites*

174 Organic polymer networks can be incorporated into the cellulose structure by binding organic
175 functional groups and reactive -OH groups on the cellulose surface. Several methods have been
176 described in the literature for the development of such polymer-cellulose nanocomposites.
177 Physical methods, such as mechanical treatment with high pressure homogenization and casting
178 of an intermediate micelle structure, can improve the tensile strength, contact angle and polymer
179 grafting of cellulose fibers (Boufi & Gandini, 2001; Miao & Hamad, 2013). Different physical and
180 chemical techniques are widely used to either attach end products of polymers (known as grafting
181 to) or allow grafting reaction to proceed from the cellulose surface (grafting from). Grafting
182 consists of one base polymer that acts as the main chain with one or more branches of long polymer
183 chains (Russell, 2002). Several techniques for grafting of polymer exist: 1) free radical grafting
184 (via chain transfer, chemical activation, γ-Ray, ultraviolet light, Plasma radiation, etc.); 2) ionic
185 and ring opening grafting; 3) direct grafting of pre-made polymers (grafting to); and 4) living
186 radical reactions for grafting (i.e., nitroxide-mediated polymerization (NMP), atom transfer radical
187 polymerizations (ATRP), reversible addition–fragmentation chain transfer polymerization
188 (RAFT)) are well described in the literature (Carlmark & Malmström, 2002; Glaied et al., 2009;
189 Guo et al., 2013; Roy et al., 2009; Russell, 2002). Recently, Alzate-Sánchez et al., reported

190 polymer grafting of cellulose microcrystals (CMCs) and cotton fabric using β-Cyclodextrin
191 (β-CD) polymers functionalized with tetrafluoroterephthalonitrile (TFN; Figure 2C) (Alzate-
192 Sánchez et al., 2019; Alzate-Sánchez et al., 2016). Here, the simultaneous formation of the CD-
193 TFN polymer and its grafting onto the cellulose precursor is performed in a solvent mixture of
194 dimethyl sulfoxide (DMSO) and H_2O (Figure 2C). Copolymerization in bacterial culture media is
195 another method that allows for facile preparation of polymer-cellulose nanocomposites.
196 Previously, alginate hydrogel beads were functionalized with CNFs (~30 nm) by cultivation of *G.*
197 *xylinus* bacteria in the presence of hydrogel beads for 36 hrs (Kim et al., 2017). Given their
198 powdered form and heterogeneous size distribution, polymers generally need a support structure
199 for implementation in commercial membranes and filtration systems where they are subjected to
200 high pressure and continuous water flow. The use of cellulose support structures with guest
201 polymers have demonstrated ~100% removal for a series of commonly found organic
202 micropollutants in water (Alzate-Sánchez et al., 2019). This illustrates the great potential of further
203 development of cellulose-polymer nanocomposites in environmental applications.

204 *2.3. Cellulose-MOF nanocomposites*

205 Metal–organic frameworks (MOFs) are highly porous crystalline materials in which metal ions are
206 connected to organic ligands to form hierarchical structures. MOFs are known for having a highly
207 porous structure that results in large surface areas and high adsorption affinity (Yang et al., 2020).
208 Given the difficulty in handling and processing of MOFs in their crystalline powdered forms, there
209 is growing research into the combination of MOFs with other materials (e.g., silica, graphene,
210 cellulose, organic polymers, etc.) for the development of MOF based nanocomposites (Rego et al.,
211 2021; Wang et al., 2019). Cellulose materials serve as templating agents with high tunability and
212 mechanical strength to support MOFs. Interfacial reactions between the functional groups of the

213 MOFs and different cellulose structures are commonly exploited to develop nanocellulose-MOF
214 nanocomposites. For example, Guo et al. combined zirconium MOF structures (UiO-66) with
215 natural wood to develop a nanocomposite membrane capable of high liquid transport and organic
216 pollutant adsorption (Figure 2D; Guo et al., 2019). The UiO-66 MOF NPs were incorporated into
217 the wood matrix by treating a solvothermal mixture of UiO-66/wood at 120 °C for 24 hrs. The
218 uniquely elongated and mesoporous wood membrane used in this study improves the contact time
219 and probability of organic pollutants with UiO-66. Therefore, further development of this low-cost
220 membrane offers immense potential in pollutant removal and other treatment applications. Zhu et
221 al. (2016). combined ZIF-8 and UiO-66 MOFs with CNC aerogels by a facile water-based sol-gel
222 process that was followed by freeze drying. The authors reported high MOF loading of up to 50
223 wt% in the aerogel structure. A high performing supercapacitor was recently reported that
224 combined a conductive MOF (Ni_3(2,3,6,7,10,11-hexaiminotriphenylene)$_2$) with CNFs (CNF@Ni–
225 HITP) via an ion-exchange reaction (Figure 2E) (Zhou et al., 2019). The resulting nanocomposites
226 exhibited high porosity, mechanical strength, and high electrical conductivity (up to 100 S cm^{-1}).
227 This reported conductivity was found to be ~5× higher than cellulose/polymer (20 S cm^{-1}) and
228 cellulose/rGO (20 S cm^{-1}), and ~10× higher than cellulose/CNTs (10 S cm^{-1}) materials (Yuan et
229 al., 2013; Xiong et al., 2016; Choi et al., 2014). These results suggest a high potential for
230 environmentally sustainable cellulose-MOF nanocomposites in the energy recovery applications.

231 3. Environmental science and engineering applications

232 In the following sections, we summarize recent advances in the application of cellulose
233 nanocomposites to address challenges in five key areas of environmental science and engineering.
234 For sensing and catalysis applications, the plasmonic (Au/Ag), magnetic (Fe_3O_4) and catalytic
235 (Au/Ag/Fe_3O_4/TiO_2) metal NPs are often utilized in metal-cellulose nanocomposites. For pollutant

236 removal, organic polymers, such as alginate, β-CD, PEDOT:PSS, carbon nanomaterials (RGO,
237 CNTs, etc.) and MOFs (ZIF-8, UiO-66, etc.) are often incorporated with cellulose nanocomposites
238 to achieve higher surface area and porosity. The use of biocompatible organic polymers (alginate,
239 chitosan, chitin, etc.) and proteins with cellulose nanocomposites are quite common in commercial
240 applications (bioplastics, tissue engineering, and food packaging). The nanocomposites discussed
241 are summarized in Table 2.

242 *3.1. Environmental sensing and detection*

243 Early detection of pollutants in environmental matrices (i.e., air, soil, water) plays an immensely
244 important role from the standpoint of public health and safety. Environmental sensing and
245 monitoring are required to inform policy and decision making and the overall protection of the
246 environment. The recent worldwide outbreak of the novel coronavirus (SARS-CoV-2) has
247 reinforced focus on wastewater-based epidemiology (WBE) (Mao et al., 2020). WBE is a
248 potentially effective way to track the spread of infection through the analysis of wastewater
249 samples for the presence of pathogenic biomarkers (Rahman et al., 2021). Nanomaterial-enabled
250 sensors are rapidly evolving as potentially cost-effective options for the rapid detection and
251 surveillance of inorganic/organic chemicals, pathogens, and other environmental pollutants
252 (Vikesland, 2018; Willner & Vikesland, 2018). Implementation of cellulose nanocomposites for
253 environmental sensing and biosensing is a growing field with an extensive body of reported
254 literature.

255 Plasmonic Au/Ag NPs can be incorporated into cellulose paper-based substrates to develop
256 SERS responsive nanocomposites. SERS sensors discriminate between target biomolecules based
257 on their unique Raman spectroscopic fingerprints (Rahman et al., 2022). SERS signals arise due
258 to the enhanced inelastic light scattering of a biomolecule when it is associated with the surface of

259 plasmonic metal NPs, such as Au or Ag. Wei et al. reported preparation of an AuNP-nanocellulose
260 based SERS substrate by *in situ* citrate reduction of Au^{3+} ions on the surface of BC hydrogels (Wei
261 et al., 2015). The substrate showed excellent SERS performance with nanomolar (~10^{-9} M)
262 detection of the herbicide atrazine and the two SERS active dyes malachite green isothiocyanate
263 (MGITC) and Rhodamine 6G. Kang et al. (2020) synthesized Au and Fe_3O_4 nanoparticle
264 functionalized BC nanocrystals (Au@Fe_3O_4@BCNCs) that combine the plasmonic properties of
265 Au and the magnetic separability of Fe_3O_4 (Figure 3A). The resulting nanocomposites were
266 dispersed in MGITC solution and exhibited sensitive (~10^{-10} M) SERS detection of MGITC in a
267 dried droplet state. Recently, Tanis et al. (2020) used Au-CNF substrates for the rapid detection of
268 *Escherichia coli* via SERS. Here, the detection assay involved the use of Au nanorods combined
269 with a SERS label ((5,5-dithiobis-(2-nitrobenzoic acid); DTNB) and antibody functionalized Au-
270 CNFs for specific binding and labeled SERS detection of *E. coli*. This SERS mapping technique
271 was sensitive up to 2 CFU mL^{-1}.

272 Cellulose paper-based substrates are often used in colorimetry, electrochemistry, and
273 visual-UV/florescence-based techniques, all of which are convenient for simple and rapid analyte
274 detection. Recently, Mako et al. (2020) reported N-(1-naphthyl)ethylenediamine (NED)
275 functionalized cellulose as a paper-based substrate for low level nitrite detection in synthetic
276 freshwater (limit of detection (LOD) ~ 0.26 μM) and real seawater (LOD ~ 0.22 μM). Here, the
277 detection mechanism involves the reaction of nitrite (if present) with two indicators, sulfanilamide
278 and NED, which forms a colored azo dye (Figure 3B). Porous cellulose membranes have been
279 combined with indicator dye (Victoria blue B) for colorimetric detection of trace amounts (LOD
280 ~ 0.01mg L^{-1}) of Cd^{II} in water by observing the gradual color change of the dye when in contact
281 with Cd^{II} ions (Jiang et al., 2020).

282 Cellulose nanomaterials are also used in paper-based microfluidic or other lateral flow
283 devices. Bhardwaj et al. (2020) developed a lateral flow immunoassay (LFI) using a nitrocellulose
284 membrane as a paper-based electrochemical immunosensor. The paper sensors were
285 functionalized with anti-influenza antibodies for rapid detection (response time <10 mins) of
286 influenza H1N1 virus (LOD ~ 2.13 PFU mL^{-1}). In another study, cellulose paper was used as a
287 platform for LFI-based detection of allergen in food samples (Hua & Lu, 2020). The detection
288 mechanism involved enrichment of target protein binding antibodies in a confined detection zone
289 (Figure 3C). Formation of protein-antibody conjugates resulted in a color change during the flow of
290 sample along the testing strip. Concentrations as low as 1 ppm ovalbumin were detected using this
291 sensor.

292 Nucleic acid-based amplification techniques are often integrated with cellulose paper-
293 based point-of-care sensors for detection of target analytes. Recently, Choopara et al. (2021)
294 reported the detection of methicillin resistant *Staphylococcus aureus* (MRSA) on a fluorometric
295 cellulose membrane paper that incorporated Loop-mediated isothermal amplification (LAMP).
296 This paper-based LAMP device exhibited ultra-low detection of the *mecA* (~10 ag) gene within 45
297 mins when incubated with a DNA fluorescent dye (Figure 3D). Yee and Sikes (2020) reported
298 colorimetric detection of biotin tagged LAMP amplicons of *Mycobacterium tuberculosis* DNA on
299 a streptavidin coated cellulose paper. This method showed detection limits of 30 copies/μL for
300 LAMP and 300 copies/μL for PCR amplification. Paper-based sensors have great potential for
301 rapid and cost-effective pathogen detection. Such sensors can be developed to operate as
302 standalone devices or in combination with conventional methods, such as enzyme-linked
303 immunosorbent assay (ELISA) and/or quantitative polymerase chain reaction (qPCR) (Rahman et
304 al., 2021).

305 These recent results call for additional experiments towards specific and lower level of
306 detection of biomarkers (i.e., (e.g., chemicals, pathogens, metabolites, etc.) in complex matrices
307 (i.e., clinical sample, wastewater, etc.) to further develop cellulose paper-based sensors. SERS
308 sensors need further research to improve heterogeneity of SERS substrates and reproducibility of
309 results. Occurrences of false negatives and difficulty in interpretation of findings remain
310 challenges for nucleic acid-based techniques. Nevertheless, advantages like device
311 miniaturization, multiplex detection, and low cost still make cellulose paper-based sensors viable
312 for future development and widespread implementation.

313

314 ### *3.2. Catalysis*

315 Metals, metal oxides, and non-metallic catalysts can be incorporated into cellulose nanomaterials
316 to develop nanocomposites suitable for catalytic applications (Alle et al., 2021; Sun et al., 2010;
317 Zhang et al., 2020). Environmental remediation using nanocellulose supported catalysts have been
318 performed under various reaction systems including catalytic reduction, photocatalysis, Fenton
319 based oxidation, etc (Ana et al., 2017; Nair et al., 2020; Wang et al., 2020).

320 Major environmental contaminants, such as synthetic dyes (e.g., methyl orange, methylene
321 blue, etc.) and certain toxic gases (e.g., NO_x), exhibit reduced toxicity as a result of catalytic
322 reduction (Alle et al., 2021; Matsumoto, 2000; Zhang et al., 2020). Noble and transition metal NPs
323 such as Au, Ag, Pd, Pt, and Cu are widely employed for reductive degradation (An et al., 2017;
324 Gholami Derami et al., 2020; Yu et al., 2021; Zhang et al., 2020). Metal NPs are often immobilized
325 on a supporting surface to prevent particle aggregation, thereby ensuring their experimental
326 stability and reusability (Gholami Derami et al., 2020; Zhang et al., 2020). AuNPs have been

327 intensely researched for their catalytic activities as a function of particle size, shape, surface-area-
328 to-volume ratio, concentration, and temperature (Chen et al., 2017; Wunder et al., 2011). Chen et
329 al. reported fabrication of 2,2,6,6-tetramethylpiperidine-1-oxyl (TEMPO)-oxidized BCNCs
330 functionalized with 4-5 nm diameter AuNPs (Chen et al., 2017). The resulting hybrid
331 nanocomposites were used as catalysts for reduction of 4-nitrophenol (4-NP) to 4-aminophenol (4-
332 AP). The BCNC supported AuNPs showed superior catalytic performance towards 4-NP reduction
333 (~20× faster) compared to unsupported AuNPs (Chen et al., 2017). Shape recoverable *in-situ*
334 grown AuNPs on TEMPO-oxidized CNCs, foam synthesized via ultrafast microwave irradiation
335 (30 s), were reported to exhibit >98% discoloration of cationic and anionic dyes over five reuse
336 cycles (Figure 4A; Alle et al., 2021). Similarly, AgNPs immobilized on hexadecyl-
337 trimethylammonium bromide (CTAB) treated CNCs exhibited significant catalytic conversion of
338 4-NP at a rate of 1.6×10^{-3} s^{-1} which was attributed to the monodisperse AgNPs in the reaction
339 suspension (An et al., 2017). Similarly, AgNP decorated CNFs crossed-linked with
340 polyethyleneimine (PEI) showed much higher 4-NP removal (3.6×10^{-3} s^{-1}) with ~98%
341 performance efficiency over 10 reuse cycles (Zhang et al., 2020). PdNPs have gained attention
342 within the scientific community owing to their high catalytic efficiency, selectivity, and low
343 dosage requirement (Gholami Derami et al., 2020; Yu et al., 2021). A PdNP decorated mesoporous
344 polydopamine embedded BC membrane exhibited >99% removal of cationic, anionic, and neutral
345 dye molecules over a wide range of pH, analyte concentrations, and multiple reuse cycles (Gholami
346 Derami et al., 2020).

347 Semiconductor photocatalysts can be used for the mineralization of persistent organic
348 contaminants. The irradiation of light with energy exceeding the band gap energy of the
349 semiconductor results in the generation of electron (e^-)/hole (h^+) pairs (Ana et al., 2017; Nair et

350 al., 2020). These e^-/h^+ pairs react with surrounding oxygen containing molecules to form reactive
351 oxygen species (ROS), such as hydroxyl ($^{\bullet}OH$) and superoxide ($O_2^{\bullet-}$) radicals, that can oxidize
352 contaminants (He et al., 2018; Nair et al., 2020). Semiconductor/cellulose nanocomposites
353 reportedly reduce the recombination rate of the photoinduced e^-/h^+ pair, thereby improving
354 contaminant removal kinetics (Jiang et al., 2020). Different kinds of inorganic semiconductors
355 have been used to produce semiconductor/cellulose nanocomposites including metal oxides (TiO_2
356 (Ana et al., 2017; Nair et al., 2020), ZnO (Lefatshe et al., 2017), CuO (Su et al., 2017)), metal
357 sulfides (CdS (Yang et al., 2011), ZnS (Pathania et al., 2015), MoS_2 (Ferreira-Neto et al., 2020)),
358 bismuth based semiconductors (BiOCl (Tian et al., 2019), BiOBr (Zhou et al., 2019), silver based
359 semiconductors (Ag@AgCl (Dai et al., 2017), Ag_3PO_4 (Lebogang et al., 2019), and non-metallic
360 nitrides (g-C_3N_4) (Chen et al., 2019). TiO_2 NPs (having a bandgap of 3.2 eV for anatase) are
361 extensively studied photocatalysts for contaminant removal due to their high thermal stability,
362 minimal-toxicity, low cost, and wide availability (Jiang et al., 2020). Sun et al. reported the
363 fabrication of TiO_2 functionalized BCNC nanocomposites that exhibited improved photocatalytic
364 degradation of methyl orange relative to the commercial photocatalyst P25 due to their larger
365 specific surface area and smaller crystallite size (Sun et al., 2010). CNCs functionalized with TiO_2
366 nanorods and Au nanocrystals extended the photocatalytic performance of TiO_2 to the visible light
367 region (Nair et al., 2020). ZnO semiconductors with a similar bandgap (3.3 eV) to TiO_2 are also
368 well studied for photocatalytic oxidation (Lefatshe et al., 2017). A ZnO functionalized cellulose
369 nanocomposite exhibited 79% photocatalytic removal of methylene blue, while pure ZnO showed
370 only 42% removal (Lefatshe et al., 2017). Likewise, CdS/BCNC nanocomposites showed efficient
371 photocatalysis performance by achieving 82% degradation of methyl orange after 90 min of solar
372 irradiation (Yang et al., 2011). Bismuth halide oxides (BiOX, X = F, Cl, Br, I) possess distinctive

373 lamellar structures, desirable bandgaps, and outstanding fluorescence properties (Jiang et al.,
374 2020). CNF doped BiOCl having a flower-like morphology exhibited complete removal of
375 Rhodamine B with 5% doping of CNFs under visible light (Figure 4B; Tian et al., 2019). Similarly,
376 flower like hybrid BiOBr/microcrystalline cellulose composites with an average pore diameter of
377 43.72 nm showed excellent photocatalytic activity with multiple reflections under visible light
378 (Zhou et al., 2019). Ag_3PO_4 has recently gained interest due to its low bandgap and desirable
379 photocatalytic activity under visible light. However, it undergoes undesirable photo-corrosion in
380 the absence of electron acceptors, thereby needing the support of compatible polymer templates
381 (Y. Jiang et al., 2020; Lebogang et al., 2019). Ag_3PO_4/cellulose nanocomposites demonstrated
382 high photocatalytic activity (~90% efficiency) under natural sunlight thus showing the good
383 compatibility between Ag_3PO_4 and nanocellulose (Lebogang et al., 2019).

384 Fenton reaction-based oxidation of contaminants is one of the most effective and widely
385 studied advanced oxidation methods. The conventional Fenton process generates •OH through the
386 reaction between ferrous (Fe^{2+}) ions and H_2O_2 over the narrow pH range of 2.0-3.0 (Divyapriya et
387 al., 2017). Fe_3O_4 is one of the more widely explored heterogenous Fenton catalysts and is effective
388 across a broader pH range while being easily recoverable. Unfortunately, pure Fe_3O_4 NPs
389 agglomerate and corrode under acidic pH conditions, thereby limiting their usage (Lu et al., 2019;
390 Zhou et al., 2020). Uniform distribution of nano-catalysts on nanocellulose can ultimately enhance
391 their catalytic activity and ensure recovery and reusability (Lu et al., 2019). Recently, Wang et al.
392 (2020) reported the application of mussel-inspired magnetic cellulose nanocomposites with
393 carboxylated CNFs as heterogenous Fenton catalysts for methylene blue degradation (Figure 4C).
394 The catalysts exhibited performance across the pH range of 2-10 with a maximum degradation
395 capacity of 2265 mg/g from pH 7-10. Sequential adsorption and oxidation of dye molecules with

396 CNFs loaded with GO–Fe (III) nanocomposite showed a 52.2% reduction in degradation
397 performance after five catalyst reuse cycles (Sajab et al., 2016). In contrast, a cellulose–GO–Fe_3O_4
398 composite exhibited only 10% performance reduction even after 20 reuse cycles thus illustrating
399 excellent recyclability (Chen et al., 2019).

400 In addition to photocatalysis and Fenton treatment, the catalytic activity of metal
401 oxide/cellulose nanocomposites in other catalytic systems has also been explored (Amiralian et
402 al., 2020; Soltani et al., 2019). Recently, Amiralian et al. (2020) reported the application of
403 magnetic cellulose nanocomposites as effective catalysts for the activation of peroxymonosulphate
404 (PMS) to remove Rhodamine B. Magnetic NPs of <20 nm and a crystallite size of 96−130 Å
405 formed on the surface of CNFs via *in situ* metal precursor hydrolysis. Approximately 94.9%
406 removal was achieved in 300 min. Sonocatalytic oxidation of tetracycline using ZnO/cellulose
407 nanocomposites was reported with ~87.6% removal achieved using the ultrasound
408 (US)/ZnO/nanocellulose system, while US/ZnO exhibited about 70% removal (Soltani et al.,
409 2019). Addition of PMS to the US/ZnO/nanocellulose system further enhanced degradation to
410 96.4%.

411 ### *3.3. Removal of environmental pollutants*

412 The surface of cellulose nanocomposites can be modified to enhance adsorption capacity towards
413 target pollutants. To achieve high removal efficiency towards metal ions, Xu et al. prepared a novel
414 tannin immobilized cellulose nanocomposite (TNCC) from wattle tannin and dialdehyde
415 nanocellulose (Xu et al., 2017). The nanocellulose was used as both the matrix and cross-linker to
416 improve the surface area while the multiple phenolic hydroxyls in the tannin molecules served as
417 adsorption sites for heavy metal ions. TNCC was used to remove Cu^{II}, Pb^{II} and Cr^{VI} ions from
418 aqueous solution. In addition to hydrophilic metal ions, nanocellulose can also be used for

419 hydrophobic pollutant removal. Rafieian et al. produced high porosity aerogels by freeze drying
420 CNFs, followed by modification with hexadecyltrimethoxylan (HDTMS) (Rafieian et al., 2018).
421 The presence of HDTMS improved CNF hydrophobicity with minimal effect on porosity. HDTMS
422 modified CNFs showed high adsorption capacities towards cooking and motor oils and could be
423 alternative adsorbents for oil spill remediation. Additional information on other variations of
424 nanocellulose based adsorbents for pollutant removal can be found elsewhere (Ji et al., 2020;
425 Zhang et al., 2019).

426 In real wastewater treatment systems, adsorbent separation and regeneration are of
427 particular interest. Recently, Rahmatika et al. developed fine particles by combining magnetic
428 Fe_3O_4 NPs and CNFs for protein adsorption (Figure 5A; Rahmatika et al., 2020). The embedded
429 Fe_3O_4 NPs enabled magnetic separation and increased the adsorbent surface area. The high
430 adsorption capacity (>950 mg/g), magnetic separation capability, and reusability enabled excellent
431 protein removal. Cellulose nanocomposites can also be used water treatment flocculants. Wang et
432 al. (2019) synthesized the microcrystalline cellulose (MCC) based amphoteric flocculant
433 MCC(pAA-co-pDMC) through graft copolymerization of MCC, ammonium chloride (DMC), and
434 acrylic acid (AA). Under neutral conditions, the negatively charged flocculant exhibited excellent
435 turbidity removal efficiency (>98%) towards positively charged kaolin (Figure 5B). Bridging and
436 aggregation of the coagulant promoted formation of large, settleable particles. The cheap,
437 nontoxic, and biodegradable cellulose-based flocculant showed great potential in removing
438 chemical oxygen demand (COD), turbidity, and color from highly turbid industrial wastewater.

439 Membrane filtration is another common process for which cellulose nanocomposites have
440 been used for pollutant removal. Gustafsson et al. successfully developed nonwoven filter papers
441 of various thickness from CNFs for wastewater treatment (Gustafsson et al., 2018). Here, the filter

442 papers exhibited high removal efficiency (>99.99%) towards even the smallest of viruses due to
443 the small pore size of 10-20 nm. Impressively, the filter papers performed well at industrially
444 relevant flow rates with good antifouling performance. The same research group developed
445 another nanocellulose based filter paper that was derived from green microalgae for real-world
446 drinking water purification in Dhaka, Bangladesh (Gustafsson et al., 2019). The highly turbid
447 source water turned completely transparent after filtration (Figure 5C). More importantly, almost
448 all the microbes detected in the feed were absent in the permeate and the PCR results showed that
449 human adenovirus DNA copies also greatly declined.

450 In addition to traditional external pressure driven membranes, nanocellulose can also be
451 applied in forward osmosis (FO) systems (Cruz-Tato et al., 2017; Fan et al., 2018). For example,
452 Cruz-Tato et al. designed thin film composite membranes to work in FO mode based on metalized
453 cellulose nanocomposites (Cruz-Tato et al., 2017). The membranes exhibited finger-like pore
454 morphologies and showed high water flux, high selectivity, and low reverse salt flux. The results
455 indicated that the fabricated membranes had high contaminant rejection in wastewater feed
456 solution. To decrease membrane biofouling, Jiang et al. (2018) creatively incorporated reduced
457 graphene oxide (RGO) flakes into a nanocellulose membrane during its growth (Figure 5D).
458 Compared with a commercial ultrafiltration membrane, the RGO/BNC membrane showed higher
459 water flux (>50 L/m^{2}h after 5 hrs) and similar contaminant rejection (~100% for 5 nm AuNPs).
460 In addition, the membrane exhibited bactericidal capabilities due to the localized surface heating
461 of RGO particles by photothermal effect.

462 Cellulose based membranes have also been used as air filters to help improve indoor air
463 quality. Liu et al. developed a soy protein isolate/cellulose (SPI/BC) based composite membrane
464 and evaluated its air filtration efficiency (Liu et al., 2017). This membrane possessed high removal

465 efficiency (>99.9%) for $PM_{2.5}$ and PM_{10} and maintained high air penetration rates (92.63%) under
466 extremely hazardous conditions. In another study, a biodegradable cellulose-MOF based filter
467 exhibited excellent filtration performance towards particulate matter, along with high gas
468 adsorption capacity (Ma et al., 2019).

469 Although tremendous progress has been made in the removal of pollutants using cellulose
470 nanocomposites, there remain some key challenges. Most of the works mentioned here are proof
471 of concept work, rather than real applications. In real water systems, various types of contaminants
472 usually coexist, and the concentration of each component depends on the corresponding water
473 environment, which poses challenges to the removal of target pollutants with high efficiency.
474 Considering variable operating and storage conditions, future material designs need to consider
475 efficient pollutant removal while maintaining the structural integrity of the cellulose
476 nanocomposites.

477 *3.4. Energy and resource recovery*

478 Although cellulose itself is not electrically conductive, the surface tunability of the material
479 enables preparation of conductive cellulose nanocomposites that can be used as electrical device
480 components. Sustainable solar energy harvesting is one of the most important energy-related
481 applications for cellulose nanocomposites and the incorporation of nanocellulose into solar cells
482 is well-developed. For example, Wang et al. (2020) fabricated flexible solar cell (FSC) electrodes
483 by depositing a conductive layer of poly(3,4-ethylenedioxythiophene):polystyrenesulfonate on
484 CNFs (Figure 6A). The introduced CNFs exhibited a significantly decreased coefficient of thermal
485 expansion of 19 ppm/K, while maintaining a transmittance of 89%@600 nm and stable
486 conductivity of ~835 S/cm. The improved thermal stability and flexibility as well as the excellent
487 transparency and conductivity of the substrate make it a promising FSC electrode. Poskela et al. ;

488 (2019) examined several different biobased cryogel membranes as electrolyte holders in dye solar
489 cells (DSC). They found that compared to a standard reference cell, membranes prepared from BC
490 can achieve 44% higher efficiency. However, the observed residual components in the
491 biomaterials (i.e., lignin in CNFs and proteins in chitin nanofibers, or ChNFs) could lead to loss
492 of charge carriers. The results of their work provide guidelines for future material selection in solar
493 cells. Instead of harvesting and long-term storage in cells for later application, solar energy can
494 also be harvested and directly applied to other fields. For example, Jiang et al. (2018) developed a
495 bilayer aerogel structure by combining CNFs with carbon nanotubes (CNT) for solar steam
496 generation. The observed solar-energy conversion efficiency (76.3%) of the CNF-CNT aerogel
497 was higher than most other reported devices for solar steam generation. Zhang et al. (2020)
498 recently developed a highly porous nanocellulose foam membrane (AGM) by combining CNTs
499 and AGM for absorbing solar energy and conversion into thermal energy. The thermal energy can
500 be further transferred for high-efficiency vapor generation, which can be applied for sea water
501 desalination.

502 Besides solar energy, other kinds of energy can be harvested using nanocellulose-based
503 devices. Li et al. (2019) successfully developed biological nanofibrous generators for energy
504 harvesting from flowing moist air (Figure 6B). The biological nanogenerators were produced from
505 charged CNFs and could be applied for moisture capture. When exposed to continuous moist air,
506 the streaming potential produced by the dynamic balance between water absorption and
507 evaporation led to an open-circuit voltage across the devices. A nanocellulose based triboelectric
508 generator (TENG) has been recently developed to harvest mechanical energy and convert it to
509 electricity. Xiong et al. (2017) reported a wearable TENG by coating hydrophobic cellulose oleoyl
510 ester NPs (HCOENPs) on a polyethylene terephthalate (PET) fabric for water energy harvesting.

511 Their results showed that the output voltage and current of the nanocomposites were 15 V and 4
512 μA under 6 mL/s flowing water. The same group also developed skin-touch-actuated textile-based
513 TENG for biomechanical energy harvesting (Xiong et al., 2018). When incorporated with
514 cloth/skin, the device can capture outputs of 60 V and 9 nC/cm^2 from subtle involuntary skin
515 friction.

516 Energy storage is another contemporary application for cellulose nanocomposites. In most
517 energy storage devices, the performance of the electrodes determines efficiency and cycle life.
518 Nanocellulose materials are widely used as substrates for the development of high stability
519 electrode materials, especially lithium-ion batteries (LIBs). Kuang et al. (2018) designed a
520 conductive nanofiber network via electrostatic assembly of neutral carbon black (CB) NPs on
521 negatively charged CNFs (Figure 6C). The uniform and continuous attachment of CB to the CNFs
522 facilitated electron transfer by increasing the contact area and decreasing the interfacial resistance.
523 The obtained electrodes exhibited superior maximum areal and volumetric energy density (30
524 mWh/cm and 538 Wh/L respectively) and excellent cycling stability (~91% capacity after 150
525 cycles). Recently, Illa et al. (2020) demonstrated a hierarchical porous carbon nanofiber anode
526 derived from BC-polyaniline (PANI) nanocomposites as a promising anode for high-rate LIBs.
527 The introduction of BC resulted in a remarkably high specific surface area (2037 m^2/g) and an
528 abundance of mesopores and micropores. The BC-PANI materials exhibited a reversible capacity
529 of 433 mAh/g with 99.5% Coulombic efficiency and a superior retention capacity of 99.1% at a
530 1C rate, making them a promising anode material for LIBs. Like LIBs, cellulose nanocomposites
531 are also used for supercapacitor electrodes. Ko et al. (2017) developed a flexible metallic cellulose
532 paper-based supercapacitor (MP-SC) with excellent energy storage performance. Porous cellulose
533 papers were used as effective reservoirs for the incorporation of high-energy pseudocapacitive

534 NPs. The metal nanoparticle layers can prevent substantial decreases in electrical conductivity.
535 The MP-SC electrode exhibited remarkable areal power density (15.1 mW/cm^2) and energy
536 density (267.3 μW h/cm^2). Besides electrodes, cellulose materials can also be used for other battery
537 components, like separators and electrolytes. Goncalves et al. (2019) developed mesoporous CNC
538 based membranes as separators for LIBs (Figure 6D). The porous 3D structure facilitated low
539 contact angle and efficient path efficiency for Li ion migration to the membrane. Furthermore, the
540 high ionic conductivity (2.7 mS/cm), electrochemical stability, and good interfacial compatibility
541 with the lithium electrode made them excellent separators for LIB applications. Yan et al. (2020)
542 reported a new type of quasi-solid electrolyte based on BC for LIBs (Figure 6E). The BC provided
543 abundant sites for attachment of ionic liquid electrolytes. Also, the -OH groups in BC molecular
544 chains could interact with anions to form hydrogen bonds, which promoted the dissociation of the
545 lithium salts. Compared with generally liquid electrolytes, this new type of electrolyte showed
546 almost the same discharge capacity of 138.4 mA h/g with a high Coulombic efficiency of ~99.9%
547 after 100 cycles of use at 0.1 C.

548 It is worth noting that the energy and resource recovery applications of cellulose
549 nanocomposites is still in the early stages. The energy harvest and storage properties of such
550 materials are highly dependent on the conductive materials on cellulose surfaces and within the
551 structures. Reproducibility and lifelong stability of the materials are considered key aspects in
552 terms of application. As such, expertise on fabrication and modification is highly needed.

553 *3.5. Sustainable commercial applications (bioplastics, tissue engineering, and*
554 *food packaging)*

555 Cellulose materials have been widely applied in food packaging, the textile industry, and
556 the medical sector for their high flexibility, biodegradability, and low cost (Blilid et al., 2020; Li
557 et al., 2020; Wu et al., 2018). Furthermore, the structure of cellulose provides mechanical strength
558 and acts as a barrier against potentially unwanted compounds. Urbina et al. (2019) synthesized a
559 composite BC by infiltrating BCNCs into BC membranes. This process led to a denser and more
560 compact 3D nano-network and provided enhanced mechanical strength and an improved oxygen
561 barrier compared to plain BC. Cellulose-based bioplastic is gaining attention as a sustainable
562 alternative to conventional plastics. Recently, chitosan-based cellulose was developed as a
563 sustainable bioplastic (Blilid et al., 2020). Chitosan has been widely used as a biomass precursor
564 for biobased packaging since it provides excellent film-forming ability (Salari et al., 2018).
565 Chitosan nanocomposites were synthesized using phosphorylated cellulose fillers and exhibited
566 enhanced thermal and mechanical performance. Hence, merging sustainable bio-based materials,
567 such as cellulose and chitosan can enhance the overall performance of the nanocomposites and
568 promote the development of the next generation of bioplastics.

569 In tissue engineering, biomaterials, such as chitin and alginate, are often used for wound
570 healing and are incorporated with other materials for enhanced mechanical strength and
571 biodegradability. Recognizing that BCNCs have high biodegradability and strong mechanical
572 strength, Wu et al. (2018) incorporated them with chitin that has been widely used in tissue
573 engineering owing to its controlled degradation by lysozymes. Regenerated chitin embedded
574 BCNC filaments showed increased mechanical performance and good biodegradability in
575 enzymatic degradation experiments. Furthermore, *in vivo* experiments with mice showed that the
576 BCNC based chitin filament improved wound healing without measurable adverse effects.
577 Alginate, another well-known biomaterial for tissue engineering, has also been successfully

578 incorporated with BCNCs and showed enhanced mechanical performance (Yan et al., 2018). It is
579 recommended to consider certain physicochemical properties, such as crosslinking groups,
580 filament type, fiber size, tensile strength, and biocompatibility when selecting carbohydrate
581 polymers for suture materials (Kara et al., 2021).

582 Cellulose nanomaterials can be readily surface functionalized with a variety of
583 antimicrobial agents to prevent bacterial growth. For food preservation, active food packaging is
584 desired to enhance the shelf life of food. Various types of cellulose-based food packaging have
585 been fabricated in combination with diverse antimicrobial agents. Li et al. (2020) used a
586 hydrophobic active cargo as an antibacterial agent and embedded them into bacterial cellulose
587 nanofibrils (BCNFs) along with protein zein NPs. The incorporation of zein NPs to BCNs
588 improved the mechanical strength and thermal stability of the resulting nanocomposites due to the
589 strong interfacial adhesion between zein NPs. Besides, zein NPs acted as effective nanocarriers
590 for encapsulation and controlled release of bioactive cargos, providing good antibacterial
591 properties. Abral et al. (2020) reported a transparent cellulose film prepared from ginger nanofiber
592 with chemical and ultra-sonification. The bioactive compounds that were released from the ginger
593 fibers showed antimicrobial activity against *Staphylococcus aureus, Bacillus subtilis, E. coli,*
594 *Pseudomonas aeruginosa, and Candida albicans*. Yordshadi et al. (2020) used secreted soluble
595 materials, known as postbiotics, from the lactic acid bacteria, *Lactobacillus*. *L. plantarum*
596 postbiotics were incorporated into BC and applied to extend the shelf life of ground beef under
597 refrigerated storage conditions. The postbiotics from *L. plantarum* were released in the bacterial
598 suspension. After centrifugation, the supernatant of the growth media was filtered and the freeze-
599 dried filtrate was used as probiotic. The probiotics-incorporated BC significantly reduced the
600 survival of the foodborne pathogen, *Listeria monocytogenes*, on the meat compared to unwrapped

601 and plain BC wrapped conditions. The overall shelf life of ground beef was increased by the
602 probiotics-incorporated BC without undesirable sensorial changes. Metal and metal oxide NPs
603 have been widely incorporated into cellulose and have shown great promise as antimicrobial
604 agents. Islam et al. (2018) reported facile and robust immobilization of AgNPs onto cellulose paper
605 using dopamine. Dopamine has a strong affinity to Ag through its catechol group. Another study
606 reported the development of transparent chitosan-AgNP-BCNC nanocomposite films (Salari et al.,
607 2018). Both types of AgNP-based cellulose papers exhibited strong antimicrobial activity against
608 highly virulent and antibiotic resistant bacterial strains. Additionally, cadmium oxide (CdO) NPs
609 were incorporated into the porous structure of TEMPO-oxidized CNFs (Mwafy et al., 2019). It
610 also showed great antimicrobial activities against tested bacteria since CdO deactivates cellular
611 enzymes and DNA by coordinating electron-donating groups. These results suggest significant
612 recent developments in cellulose nanocomposites with antimicrobial properties. However, further
613 research on preparation of protein and metal NPs, storage conditions of NPs, antimicrobial coating
614 strategies is still needed before commercial-scale production.

615 4. Conclusions and Future Outlook

616 In this review, we discussed the current state of the science regarding the different types of
617 cellulose nanomaterials, preparation methods of cellulose nanocomposites, and the application of
618 these nanocomposites across different fields. Cellulose nanomaterials can be used to develop low
619 cost and biocompatible paper-based sensors. This offers great potential for the future development
620 of point-of-use sensors for field deployment. Cellulose based nanocomposites offer great potential
621 as catalysts in environmental remediation and catalytic degradation of pollutants. Advantageous
622 properties of cellulose, such as high specific surface area, machinal and thermal durability, and
623 surface tunability can be used to develop high quality membranes for contaminant removal through

624 adsorption and filtration. Furthermore, these properties are also of use for sustainable energy
625 harvesting applications enabled through the incorporation of cellulose nanocomposites in energy
626 storage devices. The straightforward processes involved in incorporating guest materials (metals,
627 organics, MOFs, etc.) onto biocompatible cellulose have led to the rapid rise in the development
628 of sustainable commercial products in recent times. The low environmental impact and
629 biocompatibility of cellulose materials have been utilized for the development of bioplastics for
630 applications, such as food packaging, antimicrobial bandages, and tissue engineering.

631 The development and application of cellulose-based nanocomposites is a rich area of
632 research and technology. However, there remains challenges that affect the potentially expanded
633 use of such nanocomposites. The controlled growth and size distribution of metal NPs and polymer
634 networks are essential for proper functioning of the cellulose nanocomposites. For example, small
635 sized and well dispersed NPs are often desired for catalytic applications. For plasmonic Au/Ag
636 NPs, aggregated and larger NPs result in higher numbers of hot spots required for SERS
637 applications for environmental sensing. To ensure device miniaturization and portability for field
638 deployment, it is important that the nano and biomaterials used as device components function
639 properly under operating and storage conditions. The incorporation of metal NPs and organic
640 polymers may affect the biocompatibility of cellulose nanomaterials for sustainable applications.
641 Further research is needed to explore the regeneration of cellulose material to ensure recyclability
642 for repetitive applications. These challenges highlight areas with rich potential for future research
643 on developing next generation of cellulose nanocomposites for sustainable environmental
644 applications.

645

646

Acknowledgements

This research was supported by the US National Science Foundation grants OISE-1545756 and CBET-2029911. Additional support was provided by the Virginia Tech Sustainable Nanotechnology Interdisciplinary Graduate Education Program.

Disclosure Statement

No potential conflict of interest was reported by the authors.

ORCID

Peter Vikesland https://orcid.org/0000-0003-2654-5132
Asifur Rahman https://orcid.org/0000-0003-4889-7980
Wei Wang https://orcid.org/0000-0002-6231-2216
Govindaraj Divyapriya https://orcid.org/0000-0001-8668-480X
Seju Kang https://orcid.org/0000-0003-3281-4829

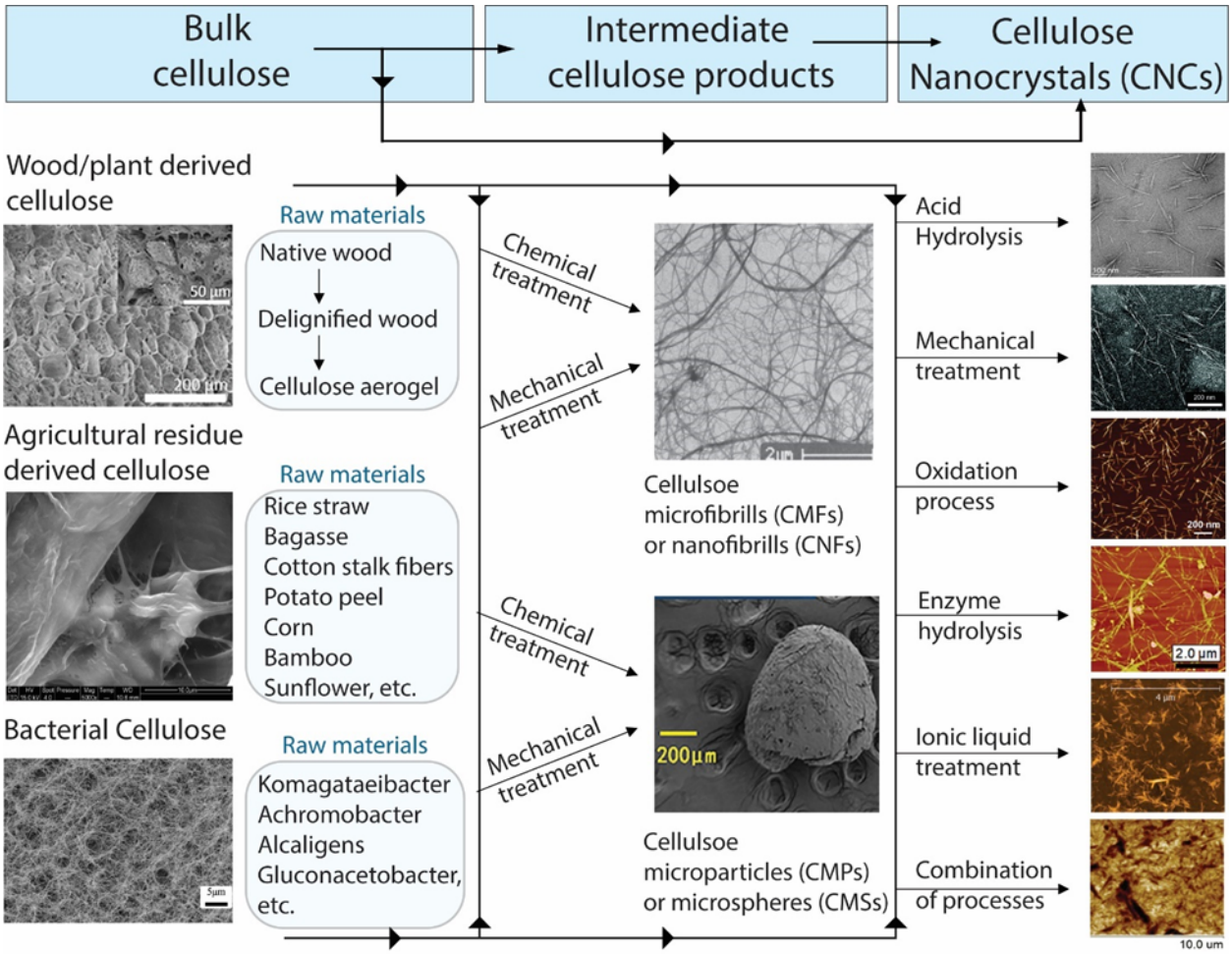

Figure 1. Types of bulk cellulose materials and their raw material sources, intermediate cellulose products derived from bulk cellulose and CNCs derived from bulk cellulose via different pathways. Images from Adel et al., 2016; Brinkmann et al., 2016; Dufresne et al., 2000; Fu et al., 2020; Garemark et al., 2020; Lee et al., 2018; G. Li et al., 2017; Pang et al., 2018; Rovera et al., 2018; Yu et al., 2021; Zhou et al., 2018.

Table 1. Summarized key information on size, specific surface area, carboxylate content, sulfate half-ester content and tensile strength of most widely used cellulose subunits. Range for the values are presented to account for the variability in reported values in the literature due to the difference in measurement conditions.

Types	Source	Size			Specific surface area (m^2/g)	-COOH loading capacity (mmol/g)	$-O-SO_3H$ loading capacity (mmol/g)	Tensile strength in mega pascals (MPa)	Ref.
		Dia. (nm)	Width (nm)	Length (µm)					
CMFs	Potato tuber cells, agricultural wastes, bulk wood	2-50	5-1000	0.2-20	30-110	1.4-1.6	0.5-2	1700-2000	(Adel et al., 2016; Dufresne et al., 2000; Fernandes et al., 2011; Janardhnan & Sain, 2006; Nakamura et al., 2019; Siró & Plackett, 2010; Spence et al., 2011; Zhang et al., 2020; Dong et al., 1998; Araki et al., 1998)
CNFs	Bleached softwood pulp, bacteria, canola straw fibers	4-64	2-70	0.1-20	150.61-201	1.12-1.43	0.2-1.8	48-10600	(Alle et al., 2021; Chen et al., 2017; Chun et al., 2011; Ji et al., 2020; Li et al., 2017; Li et al., 2020; Usov et al., 2015; Wang et al., 2020; Zhang et al., 2020; Zhang et al., 2020; Zhang et al., 2019; Camargos et al., 2021; Luo et al., 2018)
CNCs	Softwood bleached kraft pulp, bacteria	5-10	3-50	0.067-5	7.3-500	0.4-1.74	0.2-0.3	4170±1410	(Brinkmann et al., 2016; Gonçalves et al., 2019; Nair et al., 2020; Usov et al., 2015; Zhou et al., 2018; Johnston et al., 2018, Beck et al., 2015)

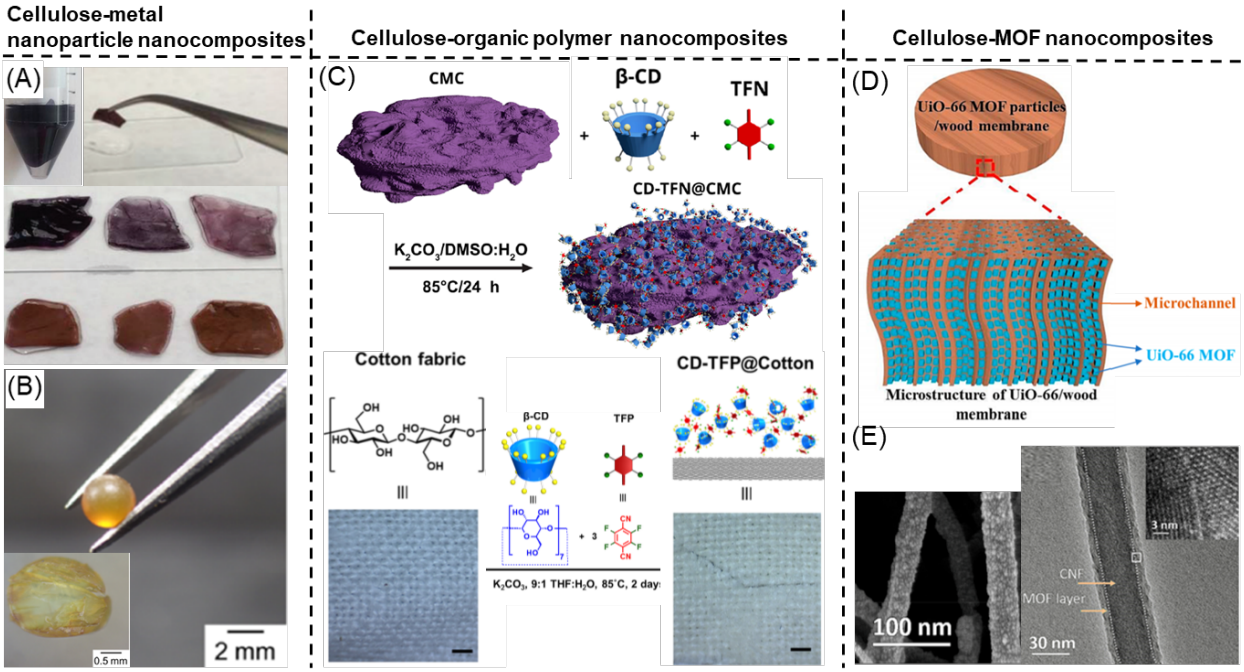

Figure 2. Different types of cellulose nanocomposites: (A) AuNP coated bulk cellulose (Wei et al., 2015), (B) AgNPs incorporated onto micro-crystalline cellulose particles with inset showing the cross-section view (Fujii et al., 2020), (C) β-CD polymerization of CMCs (top image) and cotton fabric (bottom image) (Alzate-Sánchez et al., 2019; Alzate-Sánchez et al., 2016), (D) UiO-66 MOF particles formed in the micro-structure of the wood membrane (Guo et al., 2019), I Scanning electron microscopy (SEM, in left image) and Transmission electron microscopy (TEM, in right image with inset showing a high-resolution TEM image) images of CNF@Ni–HITP nanofibers (Zhou et al., 2019).

Table 2. Summary information on previously reported applications of cellulose nanocomposites

Type of cellulose	Guest material	Application	Preparation method	Precursor used	Ref
BC	AuNPs	Sensing	Reduction by sodium citrate	$HAuCl_4$	(Wei et al., 2015)
BCNCs	Fe_3O_4+AuNPs	Sensing	Reduction in solution	$FeCl_3.6H_2O$, $FeCl_2$	(Kang et al., 2020)
CNFs	Au nanorods	Sensing	Reduction in solution	$HAuCL_4$	(Tanis et al., 2020)
Bulk cellulose	N-(1-naphthyl) Ethylenediamine	Sensing	Covalent attachment in solution	N-(1-naphthyl)-ethylenediamine·HCl	(Mako et al., 2020)
Bulk cellulose	Victoria blue B (VBB)	Sensing	Adsorption in solution	VBB solution	(Jiang et al., 2020)
CMPs	AgNPs	Catalysis	Reduction using carboxylate groups (-COOH)	$AgNO_3$	(Fujii et al., 2020)
CNFs	TiO_2	Catalysis	Mixing in dispersion and freeze drying	TiO_2 NPs	(M. Li et al., 2020)
Porous Cellulose films	TiO_2/Fe_3O_4	Catalysis	Dispersion in Ionic liquid	TiO_2/Fe_3O_4 NPs	(Wittmar et al., 2017)
CNFs	Alginate hydrogel beads	Pollutant Removal/catalysis	Copolymerization in bacterial culture media	*G. xylinus* bacteria and culture media	(Kim et al., 2017)
BCNFs	AuNPs	Catalysis	Reduction in solution	$NaBH_4$	(Chen et al., 2017)
CNCs	Fe(0)	Pollutant removal	Reduction by $NaBH_4$	$FeSO_4.7H_2O$	(Bossa et al., 2017)
CMCs, cotton fabric	β-CD polymers	Pollutant removal	Polymer grafting in solution	β-CD+TFN	(Alzate-Sánchez et al., 2019; Alzate-Sánchez et al., 2016)
Bulk cellulose (wood membrane)	Zirconium MOF (UiO-66)	Pollutant removal	Solvothermal reaction	Zirconium (Zr), Terephthalic acid (TPA)	(R. Guo et al., 2019)
CNC aerogel	ZIF-8+UiO-66 MOFs	Pollutant removal	Sol-gel process	$ZnCl_2.6H_2O$, $ZrCl_4$	(Zhu et al., 2016)
BC	Reduced graphene oxide (RGO)	Pollutant removal	in situ incorporation of GO flakes into BC	GO, *G. xylinus* bacteria and culture media	(Q. Jiang et al., 2018)
CNFs	poly(3,4-thylenedioxythiophene) :polystyrenesulfonate (PEDOT:PSS)	Energy recovery	Deposition by mixing in solution	PEDOT: PSS solution	(R. Wang et al., 2020)
Bulk cellulose aerogel	Carbon nanotubes (CNTs)	Energy recovery	Ice-templating, freeze drying and CNT coating	CNT in isopropanol	(Geng et al., 2020)
CMPs	Hydrophobic oleoyl esters	Energy recovery	Mixing in organic solvents	Oleoyl chloride	(Xiong et al., 2017)
Bulk cellulose	Au, MnO, Fe_3O_4	Energy recovery	Dipping in NP solution	$HAuCl_4.3H_2O$, $MnCl_2.4H_2O$, $Fe(acac)_3$	(Ko et al., 2017)
CNCs, CMFs	Chitosan	Bioplastics	Solution mixing and sonication	Chitosan powder	(Blilid et al., 2020)
BCNCs	Chitin	Tissue Engineering	Wet spinning	Chitin powder	(Wu et al., 2018)
BCNFs	Protein zein (ZN) NPs	Food packaging	Mixing in suspension	Zein powder, sodium caseinate	(Q. Li et al., 2020)

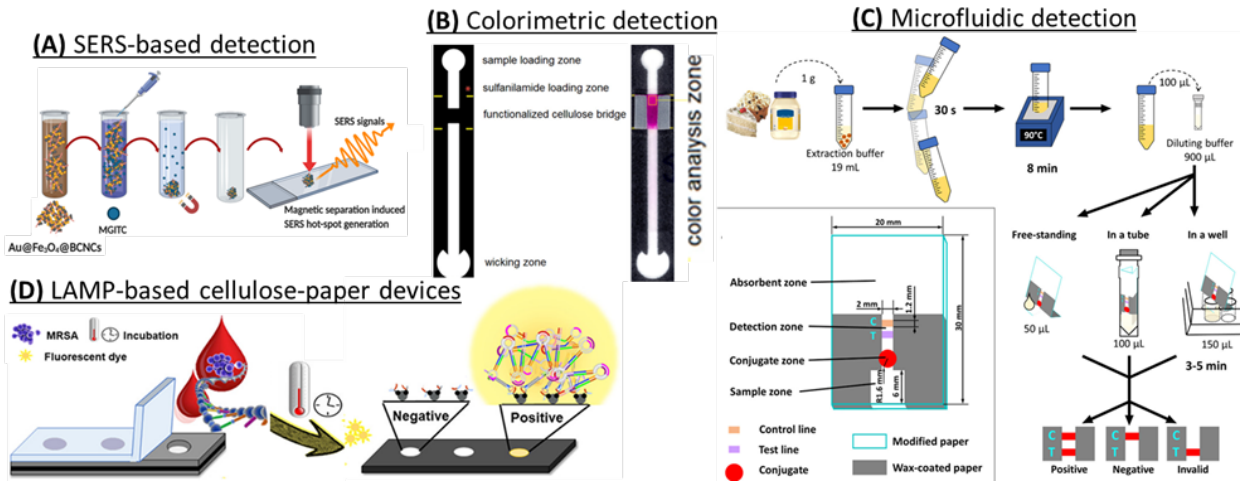

Figure 3. Environmental sensing applications of cellulose nanocomposites: (A) SERS-based sensing using Au and Fe_3O_4 coated BCNCs (Kang et al., 2020), (B) Colorimetric detection of nitrite using a N-(1-naphthyl)ethylenediamine (NED) functionalized cellulose paper-based substrate (Mako et al., 2020), (C) Allergen detection in food samples using a paper-based electrochemical immunosensor (Hua & Lu, 2020), (D) A cellulose paper-based LAMP device for *mecA* gene detection (Choopara et al. 2021).

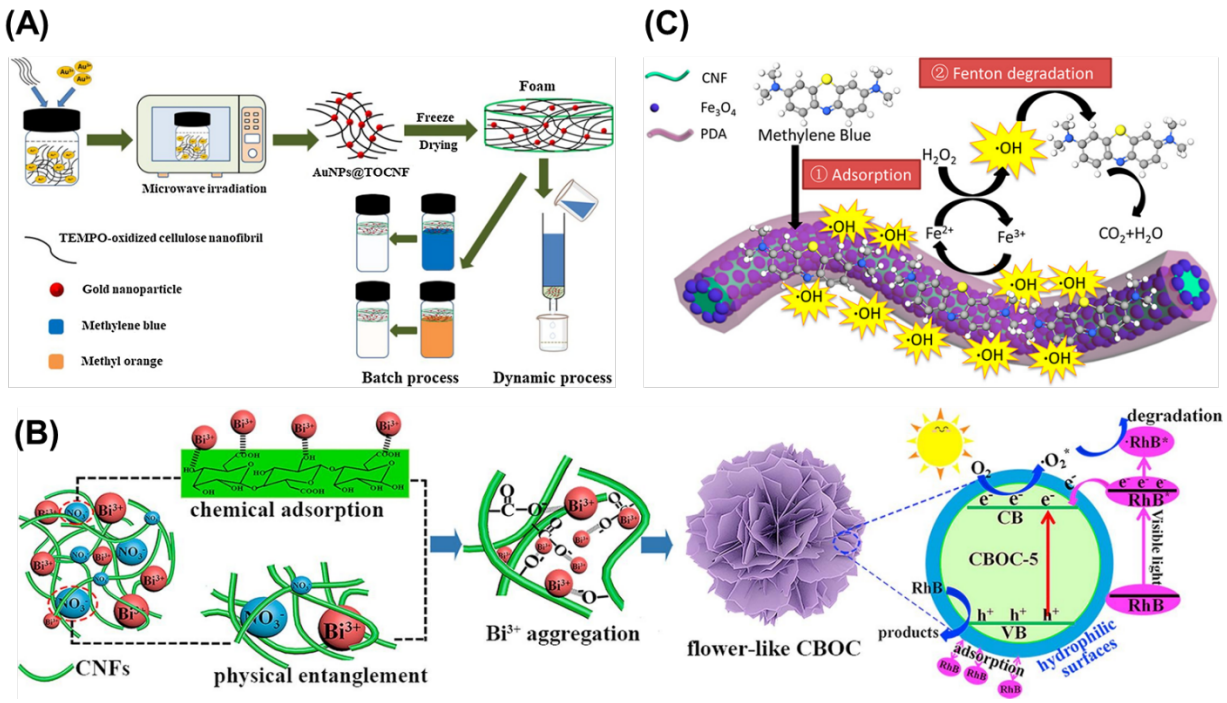

Figure 4. Catalytic applications of cellulose nanocomposites: (A) TEMPO-oxidized CNC foam for dye discoloration (Alle et al., 2021), (B) Photocatalytic removal of Rhodamine B using flower like CNF doped BiOCL (Tian et al., 2019), (C) Methylene Blue degradation using Fe_3O_4 coated CNFs as Fenton catalysts (Wang et al., 2020).

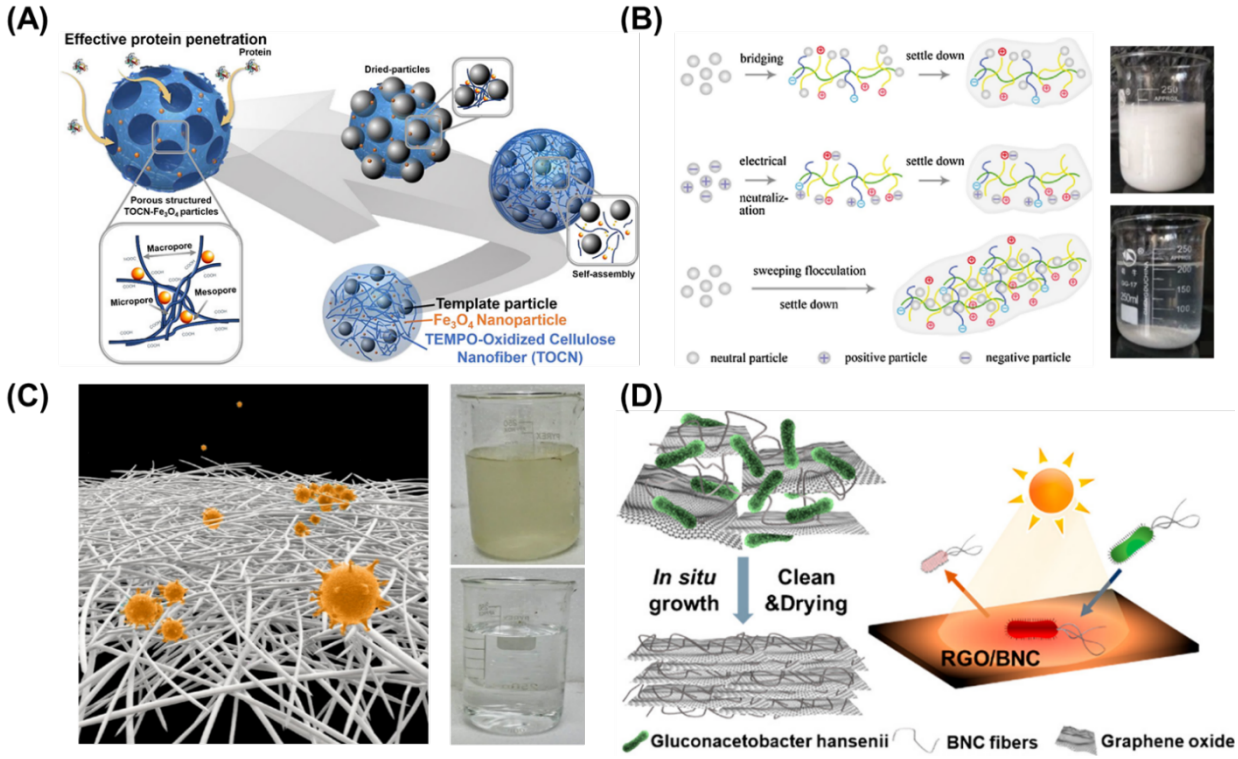

Figure 5. Pollutant removal using cellulose nanocomposites: (A) Fe_3O_4 coated CNFs for protein adsorption and removal via magnetic separation (Rahmatika et al., 2020), (B) MCC based flocculant for turbidity removal in suspension (Wang et al., 2019), (C) Nanocellulose derived filter paper for turbidity and pathogen removal in Dhaka, Bangladesh (Gustafsson et al., 2019), (D) In situ growth of RGO/BNC membrane and its application in photothermal inactivation of bacteria (Q. Jiang et al., 2018).

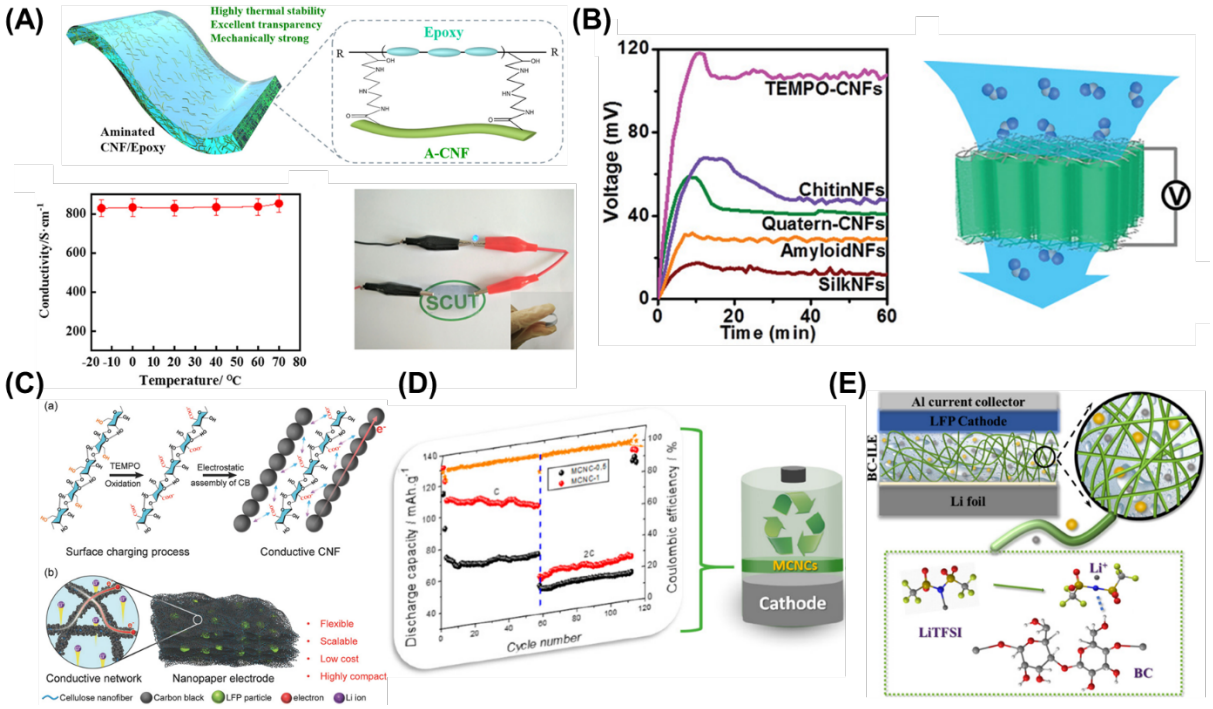

Figure 6. Cellulose nanocomposites for energy and resource recovery: (A) FSC electrodes developed using PEDOT:PSS on CNFs showing stable conductivity over a wide temperature range (Wang et al., 2020), (B) Comparison of open-circuit voltage (Voc) generated by nanocellulose and other sources derived biological nanofibrous generators. (M. Li et al., 2019), (C) Electron transfer using conductive nanocomposites of CB NPs modified CNFs (Kuang et al., 2018), (D) Cycle performance of mesoporous CNC separators for LIBs (Gonçalves et al., 2019), (E) A BC based quasi-solid electrolyte where BC provides plenty of binding sites for attachment of Lithium bis(trifluoromethanesulfonyl)imide (LiTFSI) (Yan et al., 2020).

References

1) Abral, H., Ariksa, J., Mahardika, M., Handayani, D., Aminah, I., Sandrawati, N., Pratama, A.B., Fajri, N., Sapuan, S.M., & Ilyas, R. (2020). Transparent and antimicrobial cellulose film from ginger nanofiber. *Food Hydrocolloids*, *98*, 105266. https://doi.org/10.1016/j.foodhyd. 2019. 105266
2) Adel, A. M., El-Gendy, A. A., Diab, M. A., Abou-Zeid, R. E., El-Zawawy, W. K., & Dufresne, A. (2016). Microfibrillated cellulose from agricultural residues. Part I: Papermaking application. *Industrial Crops and Products*, *93*, 161-174. https://doi.org/10.1016/j.indcrop.2016.04.043
3) Alle, M., Bandi, R., Sharma, G., Lee, S.-H., & Kim, J.-C. (2021). Shape recoverable, Au nanoparticles loaded nanocellulose foams as a recyclable catalyst for the dynamic and batch discoloration of dyes. *Carbohydrate polymers*, *258*, 117693. https://doi.org/10.1016/j.carbpol. 2021.117693
4) Alzate-Sánchez, D. M., Ling, Y., Li, C., Frank, B. P., Bleher, R., Fairbrother, D. H., Helbling, D.E., & Dichtel, W. R. (2019). β-Cyclodextrin polymers on microcrystalline cellulose as a granular media for organic micropollutant removal from water. *ACS applied materials & interfaces*, *11*(8), 8089-8096. https://doi.org/10.1021/acsami.8b22100
5) Alzate-Sánchez, D. M., Smith, B. J., Alsbaiee, A., Hinestroza, J. P., & Dichtel, W. R. (2016). Cotton fabric functionalized with a β-cyclodextrin polymer captures organic pollutants from contaminated air and water. *Chemistry of Materials*, *28*(22), 8340-8346. https://doi.org/10.1021/acs.chemmater.6b03624
6) Amiralian, N., Mustapic, M., Hossain, M. S. A., Wang, C., Konarova, M., Tang, J., Na, J., Khan, A., & Rowan, A. (2020). Magnetic nanocellulose: A potential material for removal of dye from water. *Journal of hazardous materials*, *394*, 122571. https://doi.org/10.1016/j.jhazmat. 2020.122571
7) An, X., Long, Y., & Ni, Y. (2017). Cellulose nanocrystal/hexadecyltrimethylammonium bromide/silver nanoparticle composite as a catalyst for reduction of 4-nitrophenol. *Carbohydrate polymers*, *156*, 253-258. https://doi.org/10.1016/j.carbpol.2016.08.099
8) Araki, J., Wada, M., Kuga, S., & Okano, T. (1998). Flow properties of microcrystalline cellulose suspension prepared by acid treatment of native cellulose. *Colloids and Surfaces A: Physicochemical and Engineering Aspects*, *142*(1), 75-82. https://doi.org/10.1016/S0927-7757(98)00404-X
9) Oliveira, A.C.D.M., dos Santos, M.S., Brandão, L.M., de Resende, I.T.F., Leo, I.M., Morillo, E.S., Yerga, R.M., Fierro, J.L.G., Egues, S.M.D.S., & Figueiredo, R.T. (2017). The effect of cellulose loading on the photoactivity of cellulose-TiO2 hybrids for hydrogen production under simulated sunlight. *International Journal of Hydrogen Energy*, *42*, 28747-28754. https://doi.org/10.1016/ j.ijhydene.2017.09.022
10) Beck, S., Méthot, M., & Bouchard, J. (2015). General procedure for determining cellulose nanocrystal sulfate half-ester content by conductometric titration. *Cellulose*, *22*(1), 101-116. https://doi.org/10.1007/s10570-014-0513-y
11) Bhardwaj, J., Kim, M.-W., & Jang, J. (2020). Rapid Airborne Influenza Virus Quantification Using an Antibody-Based Electrochemical Paper Sensor and Electrostatic Particle Concentrator.

Environmental science & technology, *54*(17), 10700-10712. https://doi.org/10.1021/acs.est.0c00441

12) Blilid, S., Kędzierska, M., Miłowska, K., Wrońska, N., El Achaby, M., Katir, N., Belamie, E., Alonso, B., Lisowska, K., Lahcini, M. and Bryszewska, M. (2020). Phosphorylated Micro-and Nanocellulose-Filled Chitosan Nanocomposites as Fully Sustainable, Biologically Active Bioplastics. *ACS Sustainable Chemistry & Engineering*, *8*(50), 18354-18365. https://doi.org/10.1021/acssuschemeng.0c04426
13) Bossa, N., Carpenter, A. W., Kumar, N., de Lannoy, C.-F., & Wiesner, M. (2017). Cellulose nanocrystal zero-valent iron nanocomposites for groundwater remediation. *Environmental Science: Nano*, *4*(6), 1294-1303. https://doi.org/10.1039/C6EN00572A
14) Boufi, S., & Gandini, A. (2001). Formation of polymeric films on cellulosic surfaces by admicellar polymerization. *Cellulose*, *8*(4), 303-312. https://doi.org/10.1023/A:1015137116216
15) Brinkmann, A., Chen, M., Couillard, M., Jakubek, Z. J., Leng, T., & Johnston, L. J. (2016). Correlating cellulose nanocrystal particle size and surface area. *Langmuir*, *32*(24), 6105-6114. https://doi.org/10.1021/acs.langmuir.6b01376
16) Camargos, C. H., & Rezende, C. A. (2021). Structure–Property Relationships of Cellulose Nanocrystals and Nanofibrils: Implications for the Design and Performance of Nanocomposites and All-Nanocellulose Systems. *ACS Applied Nano Materials*, *4*(10), 10505-10518. https://doi.org/10.1021/acsanm.1c02008
17) Carlmark, A., & Malmström, E. (2002). Atom transfer radical polymerization from cellulose fibers at ambient temperature. *Journal of the American Chemical Society*, *124*(6), 900-901. https://doi.org/10.1021/ja016582h
18) Carpenter, A. W., de Lannoy, C.-F., & Wiesner, M. R. (2015). Cellulose nanomaterials in water treatment technologies. *Environmental science & technology*, *49*(9), 5277-5287. https://doi.org/10.1021/es506351r
19) Chen, S., Lu, W., Han, J., Zhong, H., Xu, T., Wang, G., & Chen, W. (2019). Robust three-dimensional g-C_3N_4@cellulose aerogel enhanced by cross-linked polyester fibers for simultaneous removal of hexavalent chromium and antibiotics. *Chemical Engineering Journal*, *359*, 119-129. https://doi.org/10.1016/j.cej.2018.11.110
20) Chen, Y., Chen, S., Wang, B., Yao, J., & Wang, H. (2017). TEMPO-oxidized bacterial cellulose nanofibers-supported gold nanoparticles with superior catalytic properties. *Carbohydrate polymers*, *160*, 34-42. https://doi.org/10.1016/j.carbpol.2016.12.020
21) Chen, Y., Pötschke, P., Pionteck, J., Voit, B., & Qi, H. (2019). Fe_3O_4 Nanoparticles Grown on Cellulose/GO Hydrogels as Advanced Catalytic Materials for the Heterogeneous Fenton-like Reaction. *ACS omega*, *4*, 5117-5125. https://doi.org/10.1021/acsomega.9b00170
22) Choopara, I., Suea-Ngam, A., Teethaisong, Y., Howes, P.D., Schmelcher, M., Leelahavanichkul, A., Thunyaharn, S., Wongsawaeng, D., DeMello, A.J., Dean, D., & Somboonna, N. (2021). Fluorometric Paper-Based, Loop-Mediated Isothermal Amplification Devices for Quantitative Point-of-Care Detection of Methicillin-Resistant *Staphylococcus aureus* (MRSA). *ACS sensors*, *6*(3), 742-751. https://doi.org/10.1021/acssensors.0c01405

23) Choi, K. H., Cho, S. J., Chun, S. J., Yoo, J. T., Lee, C. K., Kim, W., Wu, Q., Park, S. B., Choi, D. H., Lee, S. Y. & Lee, S. Y. (2014). Heterolayered, one-dimensional nanobuilding block mat batteries. *Nano letters*, *14*(10), 5677-5686. https://doi.org/10.1021/nl5024029
24) Chun, S.-J., Lee, S.-Y., Doh, G.-H., Lee, S., & Kim, J. H. (2011). Preparation of ultrastrength nanopapers using cellulose nanofibrils. *Journal of Industrial and Engineering Chemistry*, *17*(3), 521-526. https://doi.org/10.1016/j.jiec.2010.10.022
25) Cruz-Tato, P., Ortiz-Quiles, E. O., Vega-Figueroa, K., Santiago-Martoral, L., Flynn, M., Díaz-Vázquez, L. M., & Nicolau, E. (2017). Metalized nanocellulose composites as a feasible material for membrane supports: design and applications for water treatment. *Environmental Science & Technology*, *51*(8), 4585-4595. https://doi.org/10.1021/acs.est.6b05955
26) Dai, L., Liu, R., Hu, L. Q., & Si, C. L. (2017). Simple and green fabrication of AgCl/Ag-cellulose paper with antibacterial and photocatalytic activity. *Carbohydrate polymers*, *174*, 450-455. https://doi.org/10.1016/j.carbpol.2017.06.107
27) Divyapriya, G., Nambi, I. M., & Senthilnathan, J. (2017). An innate quinone functionalized electrochemically exfoliated graphene/Fe_3O_4 composite electrode for the continuous generation of reactive oxygen species. *Chemical Engineering Journal*, *316*, 964-977. https://doi.org/10.1016/j.cej.2017.01.074
28) Dong, B. H., & Hinestroza, J. P. (2009). Metal nanoparticles on natural cellulose fibers: electrostatic assembly and in situ synthesis. *ACS applied materials & interfaces*, *1*(4), 797-803. https://doi.org/10.1021/am800225j
29) Dong, X. M., Revol, J. F., & Gray, D. G. (1998). Effect of microcrystallite preparation conditions on the formation of colloid crystals of cellulose. *Cellulose*, *5*(1), 19-32. https://doi.org/10.1023/A:1009260511939
30) Dufresne, A., Dupeyre, D., & Vignon, M. R. (2000). Cellulose microfibrils from potato tuber cells: processing and characterization of starch–cellulose microfibril composites. *Journal of Applied Polymer Science*, *76*(14), 2080-2092. https://doi.org/10.1002/(SICI)1097-4628(20000628)76:14<2080::AID-APP12>3.0.CO;2-U
31) Fan, X., Liu, Y., Quan, X., & Chen, S. (2018). Highly permeable thin-film composite forward osmosis membrane based on carbon nanotube hollow fiber scaffold with electrically enhanced fouling resistance. *Environmental Science & Technology*, *52*(3), 1444-1452. https://doi.org/10.1021/acs.est.7b05341
32) Fernandes, A.N., Thomas, L.H., Altaner, C.M., Callow, P., Forsyth, V.T., Apperley, D.C., Kennedy, C.J., & Jarvis, M.C. (2011). Nanostructure of cellulose microfibrils in spruce wood. *Proceedings of the National Academy of Sciences*, *108*(47), 1195-1203. https://doi.org/10.1073/pnas.1108942108
33) Ferreira-Neto, E.P., Ullah, S., da Silva, T.C., Domeneguetti, R.R., Perissinotto, A.P., de Vicente, F.S., Rodrigues-Filho, U.P. and Ribeiro, S.J. (2020). Bacterial Nanocellulose/MoS_2 Hybrid Aerogels as Bifunctional Adsorbent/Photocatalyst Membranes for *in-Flow* Water Decontamination. *ACS Applied Materials and Interfaces*, *12*, 41627-41643. https://doi.org/10.1021/acsami.0c14137

34) Fu, X., Ji, H., Wang, B., Zhu, W., Pang, Z., & Dong, C. (2020). Preparation of thermally stable and surface-functionalized cellulose nanocrystals by a fully recyclable organic acid and ionic liquid mediated technique under mild conditions. *Cellulose*, *27*(3), 1289-1299. https://doi.org/10.1007/s10570-019-02875-2
35) Fujii, Y., Imagawa, K., Omura, T., Suzuki, T., & Minami, H. (2020). Preparation of cellulose/silver composite particles having a recyclable catalytic property. *ACS Omega*, *5*(4), 1919-1926. https://doi.org/10.1021/acsomega.9b03634
36) Garemark, J., Yang, X., Sheng, X., Cheung, O., Sun, L., Berglund, L. A., & Li, Y. (2020). Top-Down Approach Making Anisotropic Cellulose Aerogels as Universal Substrates for Multi-Functionalization. *ACS Nano*, *14*(6), 7111–7120. https://doi.org/10.1021/acsnano.0c01888
37) Geng, S., Wei, J., Jonasson, S., Hedlund, J., & Oksman, K. (2020). Multifunctional carbon aerogels with hierarchical anisotropic structure derived from lignin and cellulose nanofibers for CO_2 capture and energy storage. *ACS Applied Materials & Interfaces*, *12*(6), 7432-7441. https://doi.org/10.1021/acsami.9b19955
38) Gholami Derami, H., Gupta, P., Gupta, R., Rathi, P., Morrissey, J. J., & Singamaneni, S. (2020). Palladium Nanoparticle-Decorated Mesoporous Polydopamine/Bacterial Nanocellulose as a Catalytically Active Universal Dye Removal Ultrafiltration Membrane. *ACS Applied Nano Materials*, *3*, 5437-5448. https://doi.org/10.1021/acsanm.0c00787
39) Glaied, O., Dube, M., Chabot, B., & Daneault, C. (2009). Synthesis of cationic polymer-grafted cellulose by aqueous ATRP. *Journal of Colloid and Interface Science*, *333*(1), 145-151. https://doi.org/10.1016/j.jcis.2009.01.050
40) Gonçalves, R., Lizundia, E., Silva, M. M., Costa, C. M., & Lanceros-Méndez, S. (2019). Mesoporous cellulose nanocrystal membranes as battery separators for environmentally safer lithium-ion batteries. *ACS Applied Energy Materials*, *2*(5), 3749-3761. https://doi.org/10.1021/acsaem.9b00458
41) Guo, R., Cai, X., Liu, H., Yang, Z., Meng, Y., Chen, F., Li, Y., & Wang, B. (2019). In situ growth of metal–organic frameworks in three-dimensional aligned lumen arrays of wood for rapid and highly efficient organic pollutant removal. *Environmental science & technology*, *53*(5), 2705-2712. https://doi.org/10.1021/acs.est.8b06564
42) Guo, Y., Wang, X., Shen, Z., Shu, X., & Sun, R. (2013). Preparation of cellulose-graft-poly (ε-caprolactone) nanomicelles by homogeneous ROP in ionic liquid. *Carbohydrate polymers*, *92*(1), 77-83. https://doi.org/10.1016/j.carbpol.2012.09.058
43) Gustafsson, O., Manukyan, L., Gustafsson, S., Tummala, G.K., Zaman, S., Begum, A., Alfasane, M.A., Siddique-e-Rabbani, K., & Mihranyan, A. (2019). Scalable and sustainable total pathogen removal filter paper for point-of-Use drinking water purification in Bangladesh. *ACS Sustainable Chemistry & Engineering*, *7*(17), 14373-14383. https://doi.org/10.1021/acssuschemeng.9b03905
44) Gustafsson, O., Manukyan, L., & Mihranyan, A. (2018). High-Performance Virus Removal Filter Paper for Drinking Water Purification. *Global Challenges*, *2*(7), 1800031. https://doi.org/10.1002/gch2.201800031

45) Habibi, Y., Lucia, L. A., & Rojas, O. J. (2010). Cellulose nanocrystals: chemistry, self-assembly, and applications. *Chemical reviews*, *110*(6), 3479-3500. https://doi.org/10.1021/cr900339w
46) He, W., Cai, J., Jiang, X., Yin, J.-J., & Meng, Q. (2018). Generation of reactive oxygen species and charge carriers in plasmonic photocatalytic Au@TiO_2 nanostructures with enhanced activity. *Physical Chemistry Chemical Physics*, *20*(23), 16117-16125. https://doi.org/10.1039/C8CP01978A
47) Hua, M. Z., & Lu, X. (2020). Development of a Microfluidic Paper-Based Immunoassay for Rapid Detection of Allergic Protein in Foods. *ACS sensors*, *5*, 12, 4048–4056 https://doi.org/10.1021/acssensors.0c02044
48) Illa, M. P., Pathak, A. D., Sharma, C. S., & Khandelwal, M. (2020). Bacterial Cellulose–Polyaniline Composite Derived Hierarchical Nitrogen-Doped Porous Carbon Nanofibers as Anode for High-Rate Lithium-Ion Batteries. *ACS Applied Energy Materials*, *3*(9), 8676-8687. https://doi.org/10.1021/acsaem.0c01254
49) Islam, M. S., Akter, N., Rahman, M. M., Shi, C., Islam, M. T., Zeng, H., & Azam, M. S. (2018). Mussel-inspired immobilization of silver nanoparticles toward antimicrobial cellulose paper. *ACS Sustainable Chemistry & Engineering*, *6*(7), 9178-9188. https://doi.org/10.1021/acssuschemeng.8b01523
50) Jacob, J., Haponiuk, J. T., Thomas, S., & Gopi, S. (2018). Biopolymer based nanomaterials in drug delivery systems: A review. *Materials today chemistry*, *9*, 43-55. https://doi.org/10.1016/j.mtchem.2018.05.002
51) Janardhnan, S., & Sain, M. M. (2006). Isolation of cellulose microfibrils–an enzymatic approach. *Bioresources*, *1*(2), 176-188. Retrieved from https://ojs.cnr.ncsu.edu/index.php/BioRes/article/view/BioRes_01_2_176_188_Janardnan_Sain_Isoluation_Cellulose_Microfibrils_Enzymatic
52) Ji, Y., Wen, Y., Wang, Z., Zhang, S., & Guo, M. (2020). Eco-friendly fabrication of a cost-effective cellulose nanofiber-based aerogel for multifunctional applications in Cu (II) and organic pollutants removal. *Journal of Cleaner Production*, *255*, 120276. https://doi.org/10.1016/j.jclepro.2020.120276
53) Jiang, F., Liu, H., Li, Y., Kuang, Y., Xu, X., Chen, C., Huang, H., Jia, C., Zhao, X., Hitz, E., & Zhou, Y. (2018). Lightweight, mesoporous, and highly absorptive all-nanofiber aerogel for efficient solar steam generation. *ACS applied materials & interfaces*, *10*(1), 1104-1112. https://doi.org/10.1021/acsami.7b15125
54) Jiang, Q., Ghim, D., Cao, S., Tadepalli, S., Liu, K.K., Kwon, H., Luan, J., Min, Y., Jun, Y.S., & Singamaneni, S. (2018). Photothermally active reduced graphene oxide/bacterial nanocellulose composites as biofouling-resistant ultrafiltration membranes. *Environmental science & technology*, *53*(1), 412-421. https://doi.org/10.1021/acs.est.8b02772
55) Jiang, X., Xia, J., & Luo, X. (2020). Simple, rapid, and highly sensitive colorimetric sensor strips from a porous cellulose membrane stained with Victoria blue B for efficient detection of trace Cd (II) in water. *ACS Sustainable Chemistry & Engineering*, *8*(13), 5184-5191. https://doi.org/10.1021/acssuschemeng.9b07614

56) Jiang, Y., Lawan, I., Zhou, W., Zhang, M., Fernando, G. F., Wang, L., & Yuan, Z. (2020). Synthesis, properties and photocatalytic activity of a semiconductor/cellulose composite for dye degradation-a review. *Cellulose*, *27*, 595-609. https://doi.org/10.1007/s10570-019-02851-w
57) Johnston, L. J., Jakubek, Z. J., Beck, S., Araki, J., Cranston, E. D., Danumah, C., Fox, D., Li, H., Wang, J., Mester, Z., Moores, A., Murphy, K., Rabb, A. S., Rudie, A. & Stephan, C. (2018). Determination of sulfur and sulfate half-ester content in cellulose nanocrystals: An interlaboratory comparison. *Metrologia*, *55*(6), 872. https://doi.org/10.1088/1681-7575/aaeb60
58) Joseph, B., Sagarika, V., Sabu, C., Kalarikkal, N., & Thomas, S. (2020). Cellulose nanocomposites: fabrication and biomedical applications. *Journal of Bioresources and Bioproducts*, *5*(4), 223-237. https://doi.org/10.1016/j.jobab.2020.10.001
59) Kang, S., Rahman, A., Boeding, E., & Vikesland, P. J. (2020). Synthesis and SERS application of gold and iron oxide functionalized bacterial cellulose nanocrystals (Au@Fe_3O_4@BCNCs). Analyst, 145(12), 4358-4368. https://doi.org/10.1016/j.jobab.2020.10.001
60) Kara, M., Kondiah, P. P., Marimuthu, T., & Choonara, Y. E. (2021). Advances in carbohydrate-based polymers for the design of suture materials: A review. *Carbohydrate Polymers*, *261*, 117860. https://doi.org/10.1016/j.carbpol.2021.117860
61) Kaushik, M., & Moores, A. (2016). Nanocelluloses as versatile supports for metal nanoparticles and their applications in catalysis. *Green Chemistry*, *18*(3), 622-637. https://doi.org/10.1039/C5GC02500A
62) Kim, J.H., Park, S., Kim, H., Kim, H.J., Yang, Y.H., Kim, Y.H., Jung, S.K., Kan, E., & Lee, S.H. (2017). Alginate/bacterial cellulose nanocomposite beads prepared using Gluconacetobacter xylinus and their application in lipase immobilization. *Carbohydrate polymers*, *157*, 137-145. https://doi.org/10.1016/j.carbpol.2016.09.074
63) Ko, Y., Kwon, M., Bae, W. K., Lee, B., Lee, S. W., & Cho, J. (2017). Flexible supercapacitor electrodes based on real metal-like cellulose papers. *Nature communications*, *8*(1), 1-11. https://doi.org/10.1038/s41467-017-00550-3
64) Kuang, Y., Chen, C., Pastel, G., Li, Y., Song, J., Mi, R., Kong, W., Liu, B., Jiang, Y., Yang, K., & Hu, L. (2018). Conductive cellulose nanofiber enabled thick electrode for compact and flexible energy storage devices. *Advanced Energy Materials*, *8*(33), 1802398. https://doi.org/10.1002/aenm.201802398
65) Lebogang, L., Bosigo, R., Lefatshe, K., & Muiva, C. (2019). Ag_3PO_4/nanocellulose composite for effective sunlight driven photodegradation of organic dyes in wastewater. *Materials Chemistry and Physics*, *236*, 121756. https://doi.org/10.1016/j.matchemphys.2019.121756
66) Lee, M., Heo, M. H., Lee, H., Lee, H.-H., Jeong, H., Kim, Y.-W., & Shin, J. (2018). Facile and eco-friendly extraction of cellulose nanocrystals via electron beam irradiation followed by high-pressure homogenization. *Green Chemistry*, *20*(11), 2596-2610. https://doi.org/10.1039/C8GC00577J
67) Lefatshe, K., Muiva, C. M., & Kebaabetswe, L. P. (2017). Extraction of nanocellulose and in-situ casting of ZnO/cellulose nanocomposite with enhanced photocatalytic and antibacterial activity. *Carbohydrate polymers*, *164*, 301-308. https://doi.org/10.1016/j.carbpol.2017.02.020

68) Li, G., Nandgaonkar, A. G., Habibi, Y., Krause, W. E., Wei, Q., & Lucia, L. A. (2017). An environmentally benign approach to achieving vectorial alignment and high microporosity in bacterial cellulose/chitosan scaffolds. *RSC Advances*, *7*(23), 13678-13688. https://doi.org/10.1039/C6RA26049G
69) Li, J., Bendi, R., Malla, R., Parida, K., & You, Z. (2021). Cellulose nanofibers-based green nanocomposites for water environmental sustainability: A review. *Emergent Materials*, *4*(5), 1259-1273. https://doi.org/10.1007/s42247-021-00300-8
70) Li, M., Qiu, J., Xu, J., & Yao, J. (2020). Cellulose/TiO_2-Based Carbonaceous Composite Film and Aerogel for Highly Efficient Photocatalysis under Visible Light. *Industrial & Engineering Chemistry Research*, *59*(31), 13997-14003. https://doi.org/10.1021/acs.iecr.0c01682
71) Li, M., Zong, L., Yang, W., Li, X., You, J., Wu, X., Li, Z., & Li, C. (2019). Biological nanofibrous generator for electricity harvest from moist air flow. *Advanced Functional Materials*, *29*(32), 1901798. https://doi.org/10.1002/adfm.201901798
72) Li, Q., Gao, R., Wang, L., Xu, M., Yuan, Y., Ma, L., Wan, Z., & Yang, X. (2020). Nanocomposites of bacterial cellulose nanofibrils and zein nanoparticles for food packaging. *ACS Applied Nano Materials*, *3*(3), 2899-2910. https://doi.org/10.1021/acsanm.0c00159
73) Liu, X., Souzandeh, H., Zheng, Y., Xie, Y., Zhong, W.-H., & Wang, C. (2017). Soy protein isolate/bacterial cellulose composite membranes for high efficiency particulate air filtration. *Composites Science and Technology*, *138*, 124-133. https://doi.org/10.1016/j.compscitech.2016.11.022
74) Lu, Q., Zhang, Y., Hu, H., Wang, W., Huang, Z., Chen, D., Yang, M., & Liang, J. (2019). In situ synthesis of a stable Fe_3O_4@cellulose nanocomposite for efficient catalytic degradation of methylene blue. *Nanomaterials*, *9*(2), 275 https://doi.org/10.3390/nano9020275
75) Luo, J., Semenikhin, N., Chang, H., Moon, R. J., & Kumar, S. (2018). Post-sulfonation of cellulose nanofibrils with a one-step reaction to improve dispersibility. *Carbohydrate polymers*, *181*, 247-255. http://dx.doi.org/10.1016/j.carbpol.2017.10.077
76) Ma, S., Zhang, M., Nie, J., Tan, J., Yang, B., & Song, S. (2019). Design of double-component metal–organic framework air filters with $PM_{2.5}$ capture, gas adsorption and antibacterial capacities. *Carbohydrate Polymers*, *203*, 415-422. https://doi.org/10.1016/j.carbpol.2018.09.039
77) Mako, T. L., Levenson, A. M., & Levine, M. (2020). Ultrasensitive Detection of Nitrite through Implementation of *N*-(1-Naphthyl) ethylenediamine-Grafted Cellulose into a Paper-Based Device. *ACS Sensors*, *5*(4), 1207-1215. https://doi.org/10.1021/acssensors.0c00291
78) Mao, K., Zhang, H., Pan, Y., & Yang, Z. (2020). Biosensors for wastewater-based epidemiology for monitoring public health. *Water research*, *191*, 116787. https://doi.org/10.1016/j.watres.2020.116787
79) Matsumoto, S. i. (2000). Catalytic reduction of nitrogen oxides in automotive exhaust containing excess oxygen by NO_x storage-reduction catalyst. *Cattech*, *4*(2), 102-109. https://doi.org/10.1023/A:1011951415060
80) Miao, C., & Hamad, W. Y. (2013). Cellulose reinforced polymer composites and nanocomposites: a critical review. *Cellulose*, *20*(5), 2221-2262. https://doi.org/10.1007/s10570-013-0007-3

81) Moon, R. J., Martini, A., Nairn, J., Simonsen, J., & Youngblood, J. (2011). Cellulose nanomaterials review: structure, properties and nanocomposites. *Chemical Society Reviews*, *40*(7), 3941-3994. https://doi.org/10.1039/C0CS00108B
82) Musino, D., Rivard, C., Landrot, G., Novales, B., Rabilloud, T., & Capron, I. (2021). Hydroxyl groups on cellulose nanocrystal surfaces form nucleation points for silver nanoparticles of varying shapes and sizes. *Journal of colloid and interface science*, *584*, 360-371. https://doi.org/10.1016/j.jcis.2020.09.082
83) Mwafy, E. A., Hasanin, M. S., & Mostafa, A. M. (2019). Cadmium oxide/TEMPO-oxidized cellulose nanocomposites produced by pulsed laser ablation in liquid environment: synthesis, characterization, and antimicrobial activity. *Optics & Laser Technology*, *120*, 105744. https://doi.org/10.1016/j.optlastec.2019.105744
84) Nair, S. S., Chen, J., Slabon, A., & Mathew, A. P. (2020). Converting cellulose nanocrystals into photocatalysts 47unctionalizationion with titanium dioxide nanorods and gold nanocrystals. *RSC Advances*, *10*, 37374-37381. https://doi.org/10.1039/D0RA05961G
85) Nakamura, Y., Ono, Y., Saito, T., & Isogai, A. (2019). Characterization of cellulose microfibrils, cellulose molecules, and hemicelluloses in buckwheat and rice husks. *Cellulose*, *26*(11), 6529-6541. https://doi.org/10.1007/s10570-019-02560-4
86) Nasseri, R., Deutschman, C., Han, L., Pope, M., & Tam, K. (2020). Cellulose nanocrystals in smart and stimuli-responsive materials: a review. *Materials Today Advances*, *5*, 100055. https://doi.org/10.1016/j.mtadv.2020.100055
87) Pang, Z., Wang, P., & Dong, C. (2018). Ultrasonic pretreatment of cellulose in ionic liquid for efficient preparation of cellulose nanocrystals. *Cellulose*, *25*(12), 7053-7064. https://doi.org/10.1007/s10570-018-2070-2
88) Pathania, D., Kumari, M., & Gupta, V. K. (2015). Fabrication of ZnS-cellulose nanocomposite for drug delivery, antibacterial and photocatalytic activity. *Materials and Design*, *87*, 1056-1064. https://doi.org/10.1016/j.matdes.2015.08.103
89) Peng, Z., Lin, Q., Tai, Y.-A. A., & Wang, Y. (2020). Applications of Cellulose Nanomaterials in Stimuli-Responsive Optics. *Journal of Agricultural and Food Chemistry*, *68*(46), 12940-12955. https://doi.org/10.1021/acs.jafc.0c04742
90) Poskela, A., Miettunen, K., Borghei, M., Vapaavuori, J., Greca, L.G., Lehtonen, J., Solin, K., Ago, M., Lund, P.D. and Rojas, O.J. (2019). Nanocellulose and nanochitin cryogels improve the efficiency of dye solar cells. *ACS Sustainable Chemistry & Engineering*, *7*(12), 10257-10265. https://doi.org/10.1021/acssuschemeng.8b06501
91) Rafieian, F., Hosseini, M., Jonoobi, M., & Yu, Q. (2018). Development of hydrophobic nanocellulose-based aerogel via chemical vapor deposition for oil separation for water treatment. *Cellulose*, *25*(8), 4695-4710. https://doi.org/10.1007/s10570-018-1867-3
92) Rahman, A., Kang, S., Wang, W., Garg, A., Maile-Moskowitz, A., & Vikesland, P. J. (2021). Nanobiotechnology enabled approaches for wastewater based epidemiology. *TrAC Trends in Analytical Chemistry*, *143*, 116400. https://doi.org/10.1016/j.trac.2021.116400

93) Rahman, A., Kang, S., Wang, W., Huang, Q., Kim, I., & Vikesland, P. J. (2022). Lectin-Modified Bacterial Cellulose Nanocrystals Decorated with Au Nanoparticles for Selective Detection of Bacteria Using Surface-Enhanced Raman Scattering Coupled with Machine Learning. *ACS Applied Nano Materials.* https://doi.org/10.1021/acsanm.1c02760
94) Rahmatika, A.M., Toyoda, Y., Nguyen, T.T., Goi, Y., Kitamura, T., Morita, Y., Kume, K., & Ogi, T. (2020). Cellulose Nanofiber and Magnetic Nanoparticles as Building Blocks Constructing Biomass-Based Porous Structured Particles and Their Protein Adsorption Performance. *ACS Sustainable Chemistry & Engineering*. *8*(50), 18686–18695. https://doi.org/10.1021/acssuschemeng.0c07542
95) Rego, R. M., Kuriya, G., Kurkuri, M. D., & Kigga, M. (2021). MOF based engineered materials in water remediation: Recent trends. *Journal of hazardous materials*, *403*, 123605. https://doi.org/10.1016/j.jhazmat.2020.123605
96) Rovera, C., Ghaani, M., Santo, N., Trabattoni, S., Olsson, R. T., Romano, D., & Farris, S. (2018). Enzymatic hydrolysis in the green production of bacterial cellulose nanocrystals. *ACS Sustainable Chemistry & Engineering*, *6*(6), 7725-7734. https://doi.org/10.1021/acssuschemeng.8b00600
97) Roy, D., Semsarilar, M., Guthrie, J. T., & Perrier, S. (2009). Cellulose modification by polymer grafting: a review. *Chemical Society Reviews*, *38*(7), 2046-2064. https://doi.org/10.1039/B808639G
98) Rusin, C. J., El Bakkari, M., Du, R., Boluk, Y., & McDermott, M. T. (2020). Plasmonic Cellulose Nanofibers as Water-Dispersible Surface-Enhanced Raman Scattering Substrates. *ACS Applied Nano Materials*, *3*(7), 6584-6597. https://doi.org/10.1021/acsanm.0c01045
99) Russell, K. (2002). Free radical graft polymerization and copolymerization at higher temperatures. *Progress in polymer science*, *27*(6), 1007-1038. https://doi.org/10.1016/S0079-6700(02)00007-2
100) Sajab, M.S., Chia, C.H., Chan, C.H., Zakaria, S., Kaco, H., Chook, S.W., & Chin, S.X. (2016). Bifunctional graphene oxide-cellulose nanofibril aerogel loaded with Fe(III) for the removal of cationic dye via simultaneous adsorption and Fenton oxidation. *RSC Advances*, *6*, 19819-19825. https://doi.org/10.1039/C5RA26193G
101) Salari, M., Khiabani, M. S., Mokarram, R. R., Ghanbarzadeh, B., & Kafil, H. S. (2018). Development and evaluation of chitosan based active nanocomposite films containing bacterial cellulose nanocrystals and silver nanoparticles. *Food Hydrocolloids*, *84*, 414-423. https://doi.org/10.1016/j.foodhyd.2018.05.037
102) Salas, C., Nypelö, T., Rodriguez-Abreu, C., Carrillo, C., & Rojas, O. J. (2014). Nanocellulose properties and applications in colloids and interfaces. *Current Opinion in Colloid & Interface Science, 19*(5), 383-396. https://doi.org/10.1016/j.cocis.2014.10.003
103) Siró, I., & Plackett, D. (2010). Microfibrillated cellulose and new nanocomposite materials: a review. *Cellulose*, *17*(3), 459-494. https://doi.org/10.1007/s10570-010-9405-y
104) Soltani, R. D. C., Mashayekhi, M., Naderi, M., Boczkaj, G., Jorfi, S., & Safari, M. (2019). Sonocatalytic degradation of tetracycline antibiotic using zinc oxide nanostructures loaded on nano-cellulose from waste straw as nanosonocatalyst. *Ultrasonics Sonochemistry*, *55*, 117-124.
105) https://doi.org/10.1016/j.ultsonch.2019.03.009

106) Spence, K. L., Venditti, R. A., Rojas, O. J., Habibi, Y., & Pawlak, J. J. (2011). A comparative study of energy consumption and physical properties of microfibrillated cellulose produced by different processing methods. *Cellulose*, *18*(4), 1097-1111. https://doi.org/10.1007/s10570-011-9533-z

107) Stark, N. M. (2016). Opportunities for cellulose nanomaterials in packaging films: A review and future trends. *Journal of Renewable Materials*, *4*(5), 313-326. https://doi.org/10.7569/JRM.2016.634115

108) Stenstad, P., Andresen, M., Tanem, B. S., & Stenius, P. (2008). Chemical surface modifications of microfibrillated cellulose. *Cellulose*, *15*(1), 35-45. https://doi.org/10.1007/s10570-007-9143-y

109) Su, X., Liao, Q., Liu, L., Meng, R., Qian, Z., Gao, H., & Yao, J. (2017). Cu_2O nanoparticle-functionalized cellulose-based aerogel as high-performance visible-light photocatalyst. *Cellulose*, *24*, 1017-1029. https://doi.org/10.1007/s10570-016-1154-0

110) Sun, D., Yang, J., & Wang, X. (2010). Bacterial cellulose/TiO_2 hybrid nanofibers prepared by the surface hydrolysis method with molecular precision. *Nanoscale*, *2*, 287-292. https://doi.org/10.1039/B9NR00158A

111) Tanis, S.N., Ilhan, H., Guven, B., Tayyarcan, E.K., Ciftci, H., Saglam, N., Boyaci, I.H., & Tamer, U. (2020). A disposable gold-cellulose nanofibril platform for SERS mapping. *Analytical Methods*, *12*(24), 3164-3172. https://doi.org/10.1039/D0AY00662A

112) Thomas, B., Raj, M. C., Joy, J., Moores, A., Drisko, G. L., & Sanchez, C. m. (2018). Nanocellulose, a versatile green platform: from biosources to materials and their applications. *Chemical reviews*, *118*(24), 11575-11625. https://doi.org/10.1021/acs.chemrev.7b00627

113) Tian, C., Luo, S., She, J., Qing, Y., Yan, N., Wu, Y., & Liu, Z. (2019). Cellulose nanofibrils enable flower-like BiOCl for high-performance photocatalysis under visible-light irradiation. *Applied Surface Science*, *464*, 606-615. https://doi.org/10.1016/j.apsusc.2018.09.126

114) Torres, F., Arroyo, J., & Troncoso, O. (2019). Bacterial cellulose nanocomposites: An all-nano type of material. *Materials Science and Engineering: C*, *98*, 1277-1293. https://doi.org/10.1016/j.msec.2019.01.064

115) Trache, D., Hussin, M. H., Haafiz, M. M., & Thakur, V. K. (2017). Recent progress in cellulose nanocrystals: sources and production. *Nanoscale*, *9*(5), 1763-1786. https://doi.org/10.1039/C6NR09494E

116) Urbina, L., Corcuera, M. Á., Eceiza, A., & Retegi, A. (2019). Stiff all-bacterial cellulose nanopaper with enhanced mechanical and barrier properties. *Materials Letters*, *246*, 67-70. https://doi.org/10.1016/j.matlet.2019.03.005

117) Usov, I., Nyström, G., Adamcik, J., Handschin, S., Schütz, C., Fall, A., Bergström, L. and Mezzenga, R. (2015). Understanding nanocellulose chirality and structure–properties relationship at the single fibril level. *Nature Communications*, *6*(1), 1-11. https://doi.org/10.1038/ncomms8564

118) Vikesland, P. J. (2018). Nanosensors for water quality monitoring. *Nature Nanotechnology*, *13*(8), 651-660. https://doi.org/10.1038/s41565-018-0209-9

119) Wang, G., Xiang, J., Lin, J., Xiang, L., Chen, S., Yan, B., Fan, H., Zhang, S., & Shi, X. (2020). Sustainable Advanced Fenton-like Catalysts Based on Mussel-Inspired Magnetic Cellulose

Nanocomposites to Effectively Remove Organic Dyes and Antibiotics. *ACS Applied Materials and Interfaces*, *12*, 51952-51959. https://doi.org/10.1021/acsami.0c14820

120) Wang, L., Xu, H., Gao, J., Yao, J., & Zhang, Q. (2019). Recent progress in metal-organic frameworks-based hydrogels and aerogels and their applications. *Coordination Chemistry Reviews*, *398*, 213016. https://doi.org/10.1016/j.ccr.2019.213016

121) Wang, R., Yu, H., Dirican, M., Chen, L., Fang, D., Tian, Y., Yan, C., Xie, J., Jia, D., Liu, H., & Wang, J., (2020). Highly Transparent, Thermally Stable, and Mechanically Robust Hybrid Cellulose-Nanofiber/Polymer Substrates for the Electrodes of Flexible Solar Cells. *ACS Applied Energy Materials*, *3*(1), 785-793. https://doi.org/10.1021/acsaem.9b01943

122) Wang, Z., Huang, W., Yang, G., Liu, Y., & Liu, S. (2019). Preparation of cellulose-base amphoteric flocculant and its application in the treatment of wastewater. *Carbohydrate Polymers*, *215*, 179-188. https://doi.org/10.1016/j.carbpol.2019.03.097

123) Wei, H., Rodriguez, K., Renneckar, S., Leng, W., & Vikesland, P. J. (2015). Preparation and evaluation of nanocellulose–gold nanoparticle nanocomposites for SERS applications. *Analyst*, *140*(16), 5640-5649. https://doi.org/10.1039/C5AN00606F

124) Wei, H., Rodriguez, K., Renneckar, S., & Vikesland, P. J. (2014). Environmental science and engineering applications of nanocellulose-based nanocomposites. *Environmental Science: Nano*, *1*(4), 302-316. https://doi.org/10.1039/C4EN00059E

125) Willner, M. R., & Vikesland, P. J. (2018). Nanomaterial enabled sensors for environmental contaminants. *Journal of Nanobiotechnology*, *16*(1), 1-16. https://doi.org/10.1186/s12951-018-0419-1

126) Wittmar, A. S., Fu, Q., & Ulbricht, M. (2017). Photocatalytic and magnetic porous cellulose-based nanocomposite films prepared by a green method. *ACS Sustainable Chemistry & Engineering*, *5*(11), 9858-9868. https://doi.org/10.1021/acssuschemeng.7b01830

127) Wu, H., Williams, G.R., Wu, J., Wu, J., Niu, S., Li, H., Wang, H., & Zhu, L. (2018). Regenerated chitin fibers reinforced with bacterial cellulose nanocrystals as suture biomaterials. *Carbohydrate Polymers*, *180*, 304-313. https://doi.org/10.1016/j.carbpol.2017.10.022

128) Wunder, S., Lu, Y., Albrecht, M., & Ballauff, M. (2011). Catalytic activity of faceted gold nanoparticles studied by a model reaction: Evidence for substrate-induced surface restructuring. *ACS Catalysis*, *1*, 908-916. https://doi.org/10.1021/cs200208a

129) Xiong, J., Cui, P., Chen, X., Wang, J., Parida, K., Lin, M.-F., & Lee, P. S. (2018). Skin-touch-actuated textile-based triboelectric nanogenerator with black phosphorus for durable biomechanical energy harvesting. *Nature Communications*, *9*(1), 1-9. https://doi.org/10.1038/s41467-018-06759-0

130) Xiong, J., Lin, M. F., Wang, J., Gaw, S. L., Parida, K., & Lee, P. S. (2017). Wearable All-Fabric-Based Triboelectric Generator for Water Energy Harvesting. *Advanced Energy Materials*, *7*(21), 1701243. https://doi.org/10.1002/aenm.201701243

131) Xiong, R., Hu, K., Grant, A. M., Ma, R., Xu, W., Lu, C., Zhang, X., & Tsukruk, V. V. (2016). Ultrarobust transparent cellulose nanocrystal-graphene membranes with high electrical conductivity. *Advanced Materials*, *28*(7), 1501-1509. https://doi.org/10.1002/adma.201504438

132) Xu, Q., Wang, Y., Jin, L., Wang, Y., & Qin, M. (2017). Adsorption of Cu (II), Pb (II) and Cr (VI) from aqueous solutions using black wattle tannin-immobilized nanocellulose. *Journal of Hazardous materials*, *339*, 91-99. https://doi.org/10.1016/j.jhazmat.2017.06.005

133) Yan, H., Huang, D., Chen, X., Liu, H., Feng, Y., Zhao, Z., Dai, Z., Zhang, X., & Lin, Q. (2018). A novel and homogeneous scaffold material: preparation and evaluation of alginate/bacterial cellulose nanocrystals/collagen composite hydrogel for tissue engineering. *Polymer Bulletin*, *75*(3), 985-1000. https://doi.org/10.1007/s00289-017-2077-0

134) Yan, M., Qu, W., Su, Q., Chen, S., Xing, Y., Huang, Y., Chen, N., Li, Y., Li, L., Wu, F., & Chen, R. (2020). Biodegradable Bacterial Cellulose-Supported Quasi-Solid Electrolyte for Lithium Batteries. *ACS Applied Materials & Interfaces*, *12*(12), 13950-13958. https://doi.org/10.1021/acsami.0c00621

135) Yang, J., Yu, J., Fan, J., Sun, D., Tang, W., & Yang, X. (2011). Biotemplated preparation of CdS nanoparticles/bacterial cellulose hybrid nanofibers for photocatalysis application. *Journal of Hazardous Materials*, *189*, 377-383. https://doi.org/10.1016/j.jhazmat.2011.02.048

136) Yang, Q., Zhang, M., Song, S., & Yang, B. (2017). Surface modification of PCC filled cellulose paper by MOF-$_5$ ($Zn_3(BDC)_2$) metal–organic frameworks for use as soft gas adsorption composite materials. *Cellulose*, *24*(7), 3051-3060. https://doi.org/10.1007/s10570-017-1331-9

137) Yang, Z., Asoh, T.-A., & Uyama, H. (2020). A cellulose monolith supported metal/organic framework as a hierarchical porous material for a flow reaction. *Chemical Communications*, *56*(3), 411-414. https://doi.org/10.1039/C9CC08232H

138) Yee, E. H., & Sikes, H. D. (2020). Polymerization-based amplification for target-specific colorimetric detection of amplified *Mycobacterium tuberculosis* DNA on cellulose. *ACS Sensors*, *5*(2), 308-312. https://doi.org/10.1021/acssensors.9b02424

139) Yordshahi, A. S., Moradi, M., Tajik, H., & Molaei, R. (2020). Design and preparation of antimicrobial meat wrapping nanopaper with bacterial cellulose and postbiotics of lactic acid bacteria. *International Journal of Food Microbiology*, *321*, 108561. https://doi.org/10.1016/j.ijfoodmicro.2020.108561

140) Yu, Y., Liu, S., Pei, Y., & Luo, X. (2021). Growing Pd NPs on cellulose microspheres via in-situ reduction for catalytic decolorization of methylene blue. *International Journal of Biological Macromolecules*, *166*, 1419-1428. https://doi.org/10.1016/j.ijbiomac.2020.11.021

141) Yuan, L., Yao, B., Hu, B., Huo, K., Chen, W., & Zhou, J. (2013). Polypyrrole-coated paper for flexible solid-state energy storage. *Energy & Environmental Science*, *6*(2), 470-476. https://doi.org/10.1039/C2EE23977A

142) Zhang, F., Li, Y., Cai, H., Liu, Q., & Tong, G. (2020). Processing nanocellulose foam into high-performance membranes for harvesting energy from nature. *Carbohydrate Polymers*, *241*, 116253. https://doi.org/10.1016/j.carbpol.2020.116253

143) Zhang, W., Wang, X., Zhang, Y., van Bochove, B., Mäkilä, E., Seppälä, J., Xu, W., Willför, S., & Xu, C. (2020). Robust shape-retaining nanocellulose-based aerogels decorated with silver nanoparticles for fast continuous catalytic discoloration of organic dyes. *Separation and Purification Technology*, *242*, 116523. https://doi.org/10.1016/j.seppur.2020.116523

144) Zhang, X.-F., Feng, Y., Wang, Z., Jia, M., & Yao, J. (2018). Fabrication of cellulose nanofibrils/UiO-66-NH_2 composite membrane for CO_2/N_2 separation. *Journal of Membrane Science*, *568*, 10-16. https://doi.org/10.1016/j.memsci.2018.09.055

145) Zhang, X., Elsayed, I., Navarathna, C., Schueneman, G. T., & Hassan, E. B. (2019). Biohybrid hydrogel and aerogel from self-assembled nanocellulose and nanochitin as a high-efficiency adsorbent for water purification. *ACS Applied Materials & Interfaces*, *11*(50), 46714-46725. https://doi.org/10.1021/acsami.9b15139

146) Zhou, S., Kong, X., Zheng, B., Huo, F., Strømme, M., & Xu, C. (2019). Cellulose nanofiber@ conductive metal–organic frameworks for high-performance flexible supercapacitors. *ACS Nano*, *13*(8), 9578-9586. https://doi.org/10.1021/acsnano.9b04670

147) Zhou, W., Sun, S., Jiang, Y., Zhang, M., Lawan, I., Fernando, G.F., Wang, L., & Yuan, Z. (2019). Template in situ synthesis of flower-like BiOBr/microcrystalline cellulose composites with highly visible-light photocatalytic activity. *Cellulose*, *26*, 9529-9541. https://doi.org/10.1007/s10570-019-02722-4

148) Zhou, Y., Saito, T., Bergström, L., & Isogai, A. (2018). Acid-free preparation of cellulose nanocrystals by TEMPO oxidation and subsequent cavitation. *Biomacromolecules*, *19*(2), 633-639. https://doi.org/10.1021/acs.biomac.7b01730

149) Zhou, Y., Shen, J., Bai, Y., Li, T., & Xue, G. (2020). Enhanced degradation of Acid Red 73 by using cellulose-based hydrogel coated Fe_3O_4 nanocomposite as a Fenton-like catalyst. *International Journal of Biological Macromolecules*, *152*, 242-249. https://doi.org/10.1016/j.ijbiomac.2020.02.200

150) Zhu, H., Yang, X., Cranston, E. D., & Zhu, S. (2016). Flexible and Porous Nanocellulose Aerogels with High Loadings of Metal–Organic-Framework Particles for Separations Applications. *Advanced Materials*, *28*(35), 7652-7657. https://doi.org/10.1002/adma.201601351